



# STATES ESTIMATION OF LITHIUM ION BATTERY USING DATA DRIVEN METHODS

Dhakal Amrit  
2023280024

Master of Science in Aeronautical and Astronautical Technologies

Prof. Wu Yu

School of Civil Aviation

Northwestern Polytechnical University  
M.Sc. Thesis Proposal presentation

# RESEARCH ROADMAP

Research Plan	Starting and ending dates	Completed content
	2024.9-2025.1	Literature review, research topic selection and proposal report
	2024.2-2025.4	Online datasets collection and experimental dataset collection using battery cycling, Electrochemical Impedance Spectroscopy(EIS) measurement of selected cells and preparation for modelling
	2025.5-2025.07	Modeling, parameter identification, and SOC/SOH joint estimation research using Equivalent Circuit Model and data driven methods for lithium batteries
	2025.08-2025.010	Building a simulation environment for an electric vehicle in Matlab/Simulink and integrating it with the battery models in Matlab for BEV simulation, which can take driving profile and ambient temperature as an input and provides battery states SOC, SOH, etc as an output.
	2025.11-2026.01	Write the graduation thesis and prepare for final defense

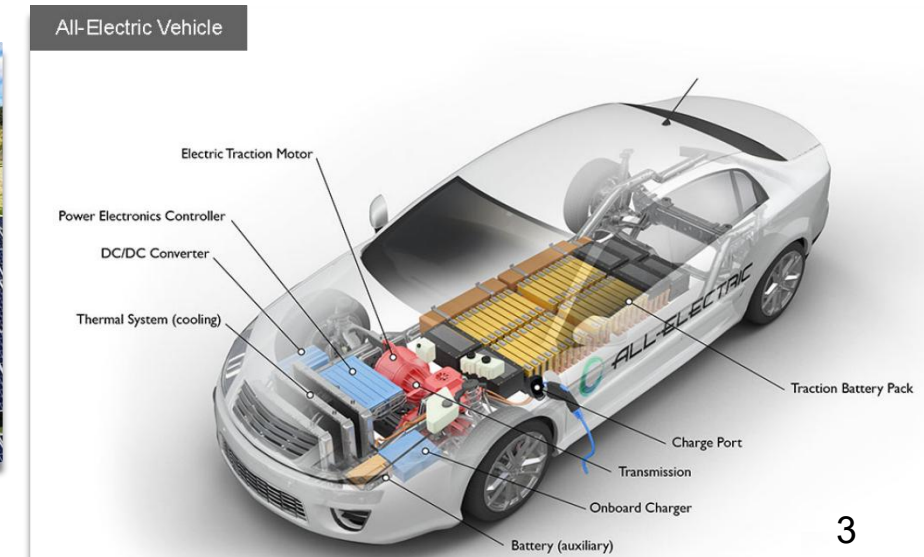
# Background



- Energy in electrical form is considered to be in its **high quality** form because it can be easily used **to control** the other forms of energy and **can be converted** very efficiently **into any other form of energy**
- Energy storage systems are required to compensate the mismatch created in supply and demand.
- At smaller level like wind power generation, and photovoltaic/solar power and electrical vehicles, the battery energy storage systems (BESS) are used for energy storage



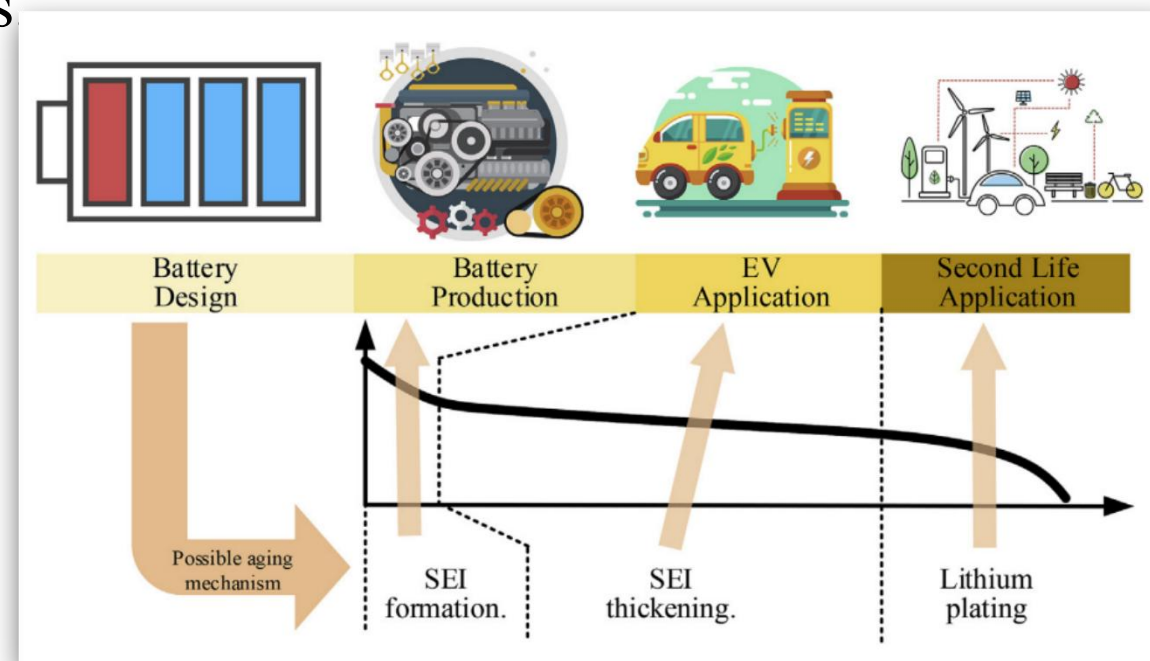
2/17/2025



# Background



- Lithium ion Battery(LIB) was first commercialized by Sony in 1991 ,
- High energy and power density, high efficiency, and rather a long lifetime
- LIBs plays a vital role in the energy transition
- They help integrate renewable energy sources (RESS), provide ancillary services, and reduce transportation emissions



Battery whole life cycle: design, production, EV application and second life application

# Background



- LIBs are also widely used in the mobile device industry, aerospace and aviation industry, and defense industry.
- All of these contribute to a rapidly increasing LIB market. However, despite its growing market and relatively good performance, climate change and particularly electric vehicle (EV) applications push for lower costs and higher energy densities over a long lifetime. Unfortunately, these metrics are generally tradeoffs, and therefore, **understanding battery aging and modeling is critical** for optimizing LIB performance.

Technology	Specific Energy (Wh/kg)		Cycle Life (number)	
	State-of-the-art	Future projection	State-of-the-art	Future projection
Ni-Cd battery	50-60	-	2000-2500	-
Li-ion battery	100-265	450	>300	400-450
Li-S battery	250-300	800-950	-	1000
Li-air battery	300-350	1300-1600	>50	500
Supercapacitor	5-15	200-300	$\infty$	$\infty$
Fuel cell	100*	500*	-	-

\*Specific power (W/kg)

# Table of Contents



CHAPTER	TOPICS
1	Lithium ion Batteries
2	Battery Management Systems(BMS)
3	Battery modelling and states estimation techniques
4	Deep Neural Network(DNN) based states estimation
5	Preliminary work- Experiments and Simulation



# 1. Lithium ion Batteries

Introduction  
Electrodes  
Electrolyte and Separator

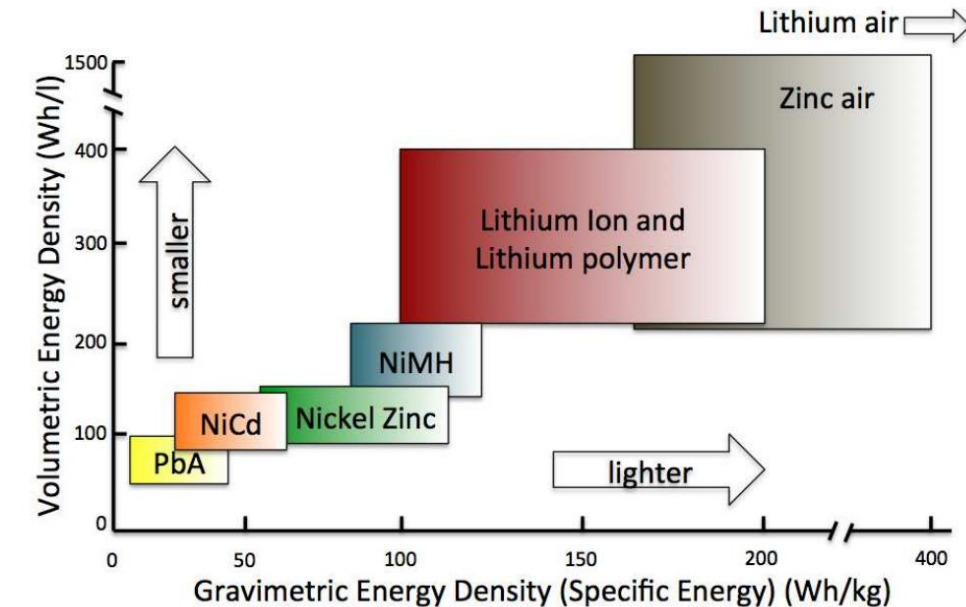
# 1.1 Lithium Ion Batteries



- **Cells** are the smallest individual electrochemical unit, and deliver a **voltage** that depends on the **cell chemistry**.
- **Cell Types**: Primary (Non rechargeable) , Secondary(Rechargeable)
- Batteries and battery packs are made up from groups of cells.



	Cylindrical cell	Prismatic cell	Pouch cell
Design for manufacture	★★ Easy for cell manufacture; Hard for pack manufacture	★★★ Hard for cell manufacture; Easy for pack manufacture	★★★ Easy for cell manufacture, Little hard for pack manufacture
Thermal characteristic	★ Poor heat dissipation since relatively low specific surface area	★★ Specific surface area related to the capacity	★★★ Usually large surface area.
Capacity Density	★★ High.	★★ Depends on cell capacity	★★★ High.
Life	★ Usually less deformation but huge stress and less electrolyte.	★★★ Usually more electrolyte.	★★★ Usually poor electrolyte, uniform deformation.
Safety	★★ Usually little capacity.	★ Usually large capacity and easy to explode.	★★★ Usually no explosion.
Cell to Module Efficiency	★ Low efficiency, hard to design TMS.	★★★ High efficiency, Easy to design TMS.	★★ Low efficiency, easy to design TMS.



# 1.2 Electrotodes

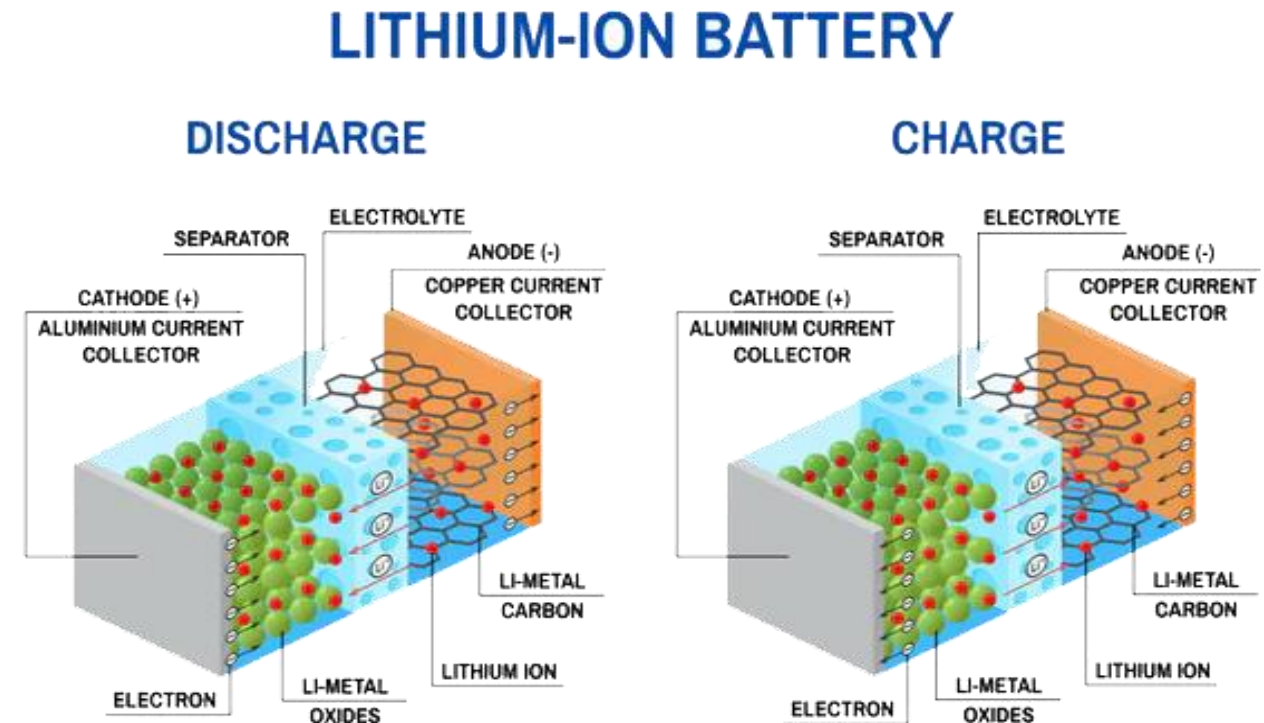


- **Negative electrode:**

1. Graphite( $C_6$ )
2. Lithium titanate Oxide ( $Li_4Ti_5O_{12}$ ) or LTO
3. Silicon etc

- **Positive electrode:**

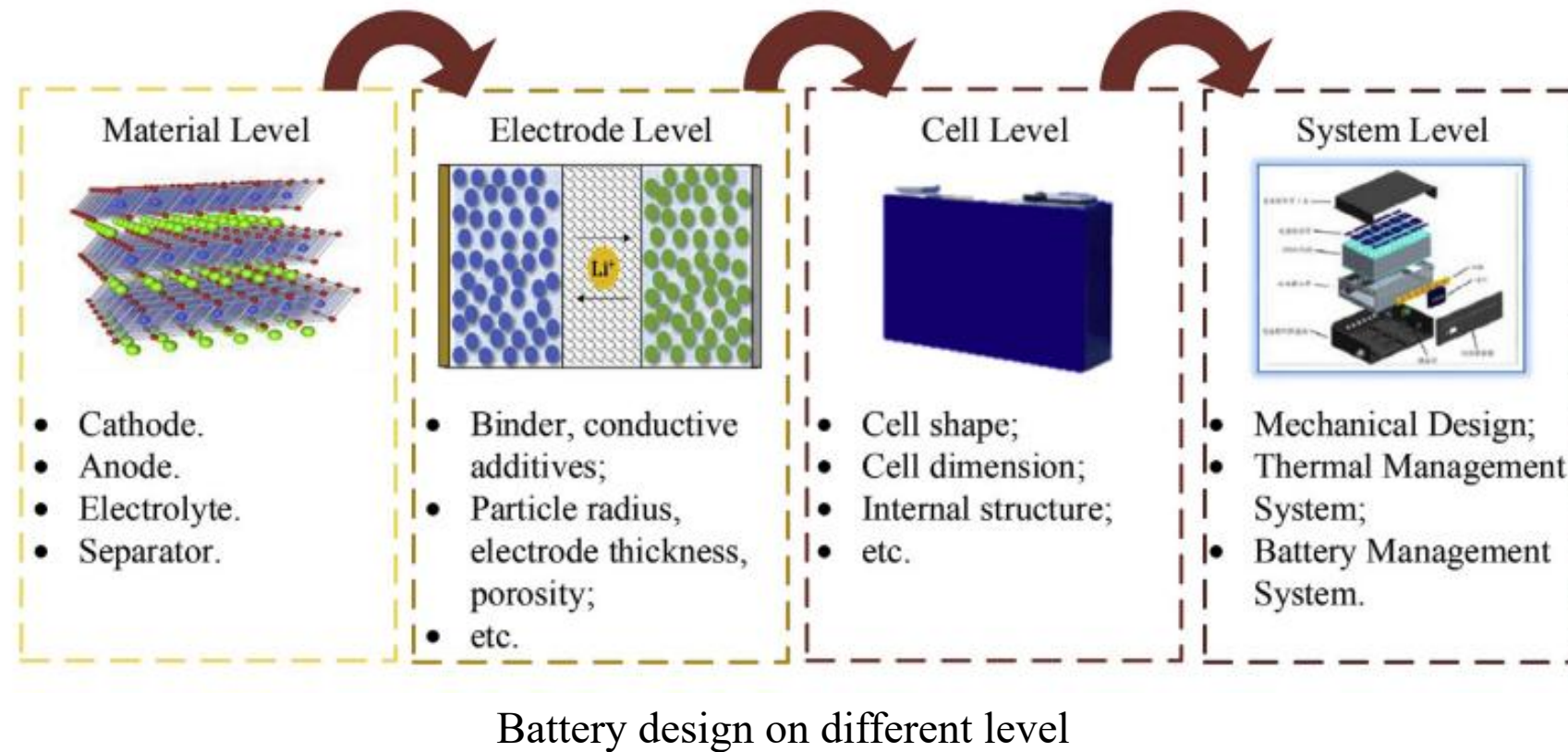
1. Lithium cobalt oxide ( $Li_xC_oO$ ) or LCO - portable electronics
2. Lithium manganese oxide ( $Li_xMn_2O_4$ , or LMO) - less expensive
3. Lithium iron phosphate ( $Li_xFePO_4$ , or LFP) - material's low-cost, low-toxicity, and very stable voltage profile



# 1.3 Electrolyte and Separator



- Electrolyte: comprises of **nonaqueous organic solvents** plus a **lithium salt** eg: lithium hexafluorophosphate ( $\text{LiPF}_6$ )
- Separator: **permeable membrane** with holes large enough to let **lithium ions pass but not the positive and negative electrode material**, it is order of  $20 \mu\text{m}$  thick; pore size is on the order of  $50 \text{ \AA}$ ;





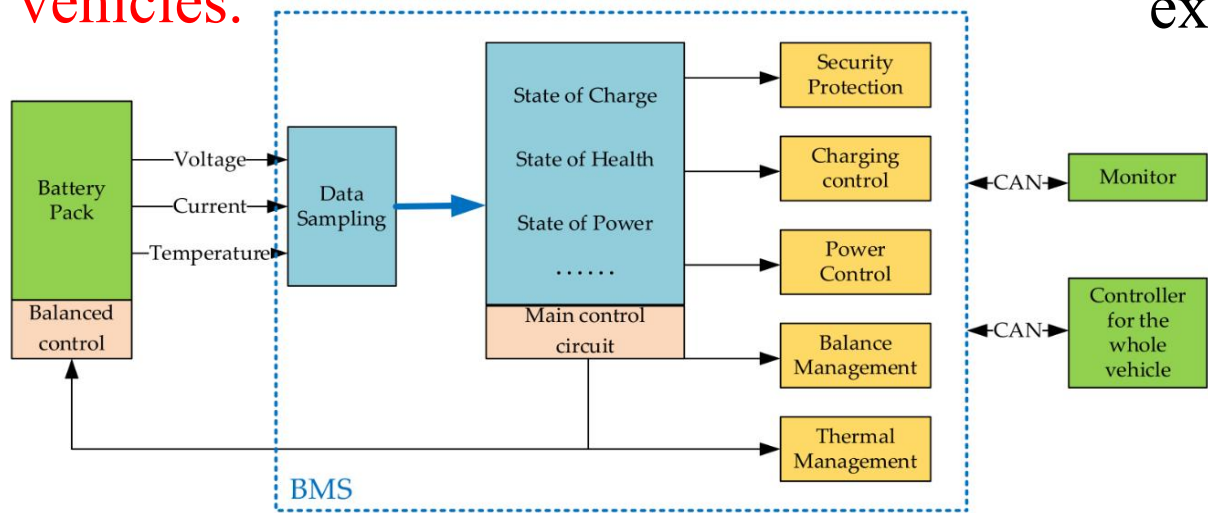
## 2. Battery Management System

Introduction  
BMS algorithm and simulation

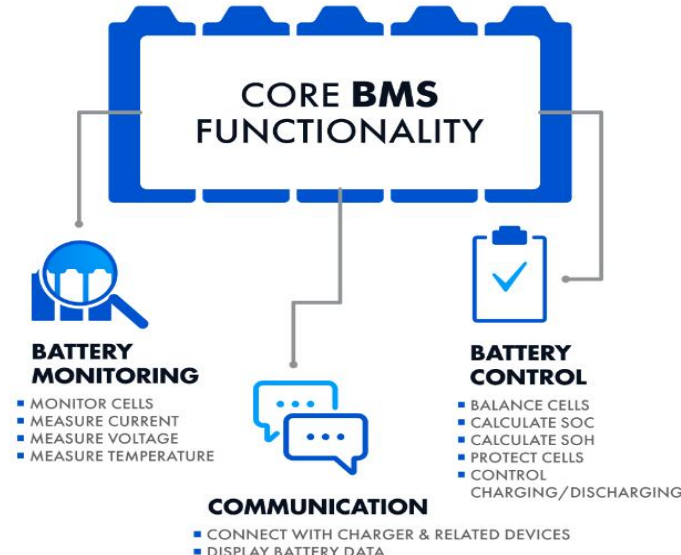
# 2.1 Battery Management System(BMS)



- BMS is an electronic system responsible for the correct and safe operation of a rechargeable battery
- A BMS finds a use in a wide range of electronics: from consumer devices, like smartphones, to life-critical medical equipment and electric vehicles.



- Battery management systems monitor and optimize battery charge and discharge cycles to help ensure battery performance, longevity, and protection from damage.
- Thus, according to Spherical Insights, the global BMS market will grow more than sixfold in the next decade, from \$7.9 billion in 2022 to an expected \$48.4 billion by 2032.



## 2.2 BMS Algorithms and Simulation



- Simulation makes it possible to reproduce the behavior of the battery and its operating environment. **Battery models** are implemented with the **help of different algorithms** that serve as estimators.
- By developing BMS software with simulation, we can create a more accurate mathematical model used for battery state estimation. Models are built using **MATLAB, GNU Octave, and other simulation software**.
- **Artificial intelligence and cloud network development** have brought new battery state estimation methods, especially suitable for severe operating conditions.



### Current & Voltage Protection

Protects the battery pack from over-charge and over-discharge thereby extending cycle life



### Health Monitoring

Monitors internal resistance of individual cells and the measured capacity of the battery pack



### Thermal Management

Over-temperature and under-temperature protection with fan controls for cooling or heating



### State of Charge Monitoring With Drift

Coulomb counting and dynamic drift correction are used to monitor the state of charge



### Digital & Analog Output Controls

Provides multiple methods of controlling chargers, motor controllers and other external devices



### Compatible With Almost All Li-Ion Batteries

A wide cell voltage range supports almost all lithium ion batteries and even some NiMH batteries



### Intelligent Cell Balancing

Efficient passive balancing is used to maximize the usable capacity of battery packs



### Field Programmable

Parameters such as voltage ranges, current limits and many other settings are easily field changeable.



### 3. Battery modelling and states estimation techniques

Battery modelling techniques

Equivalent Circuit Model

Physics based Model

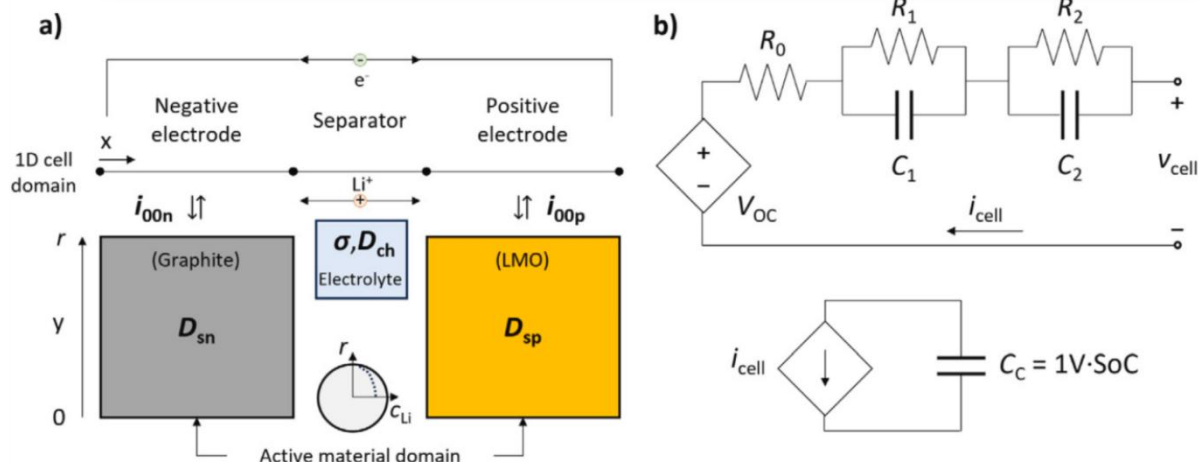
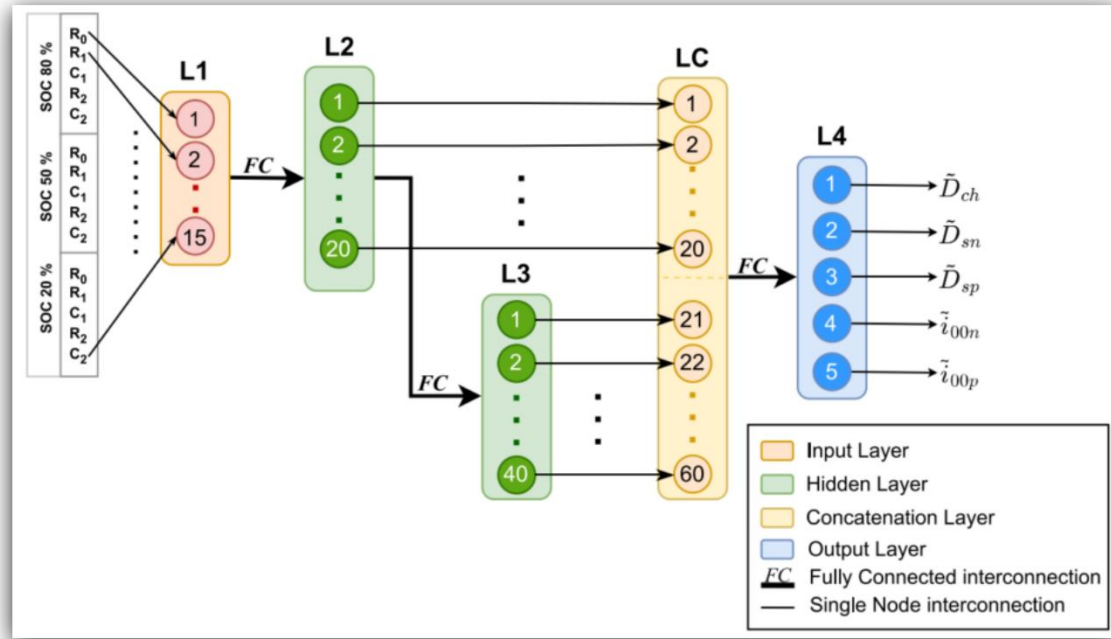
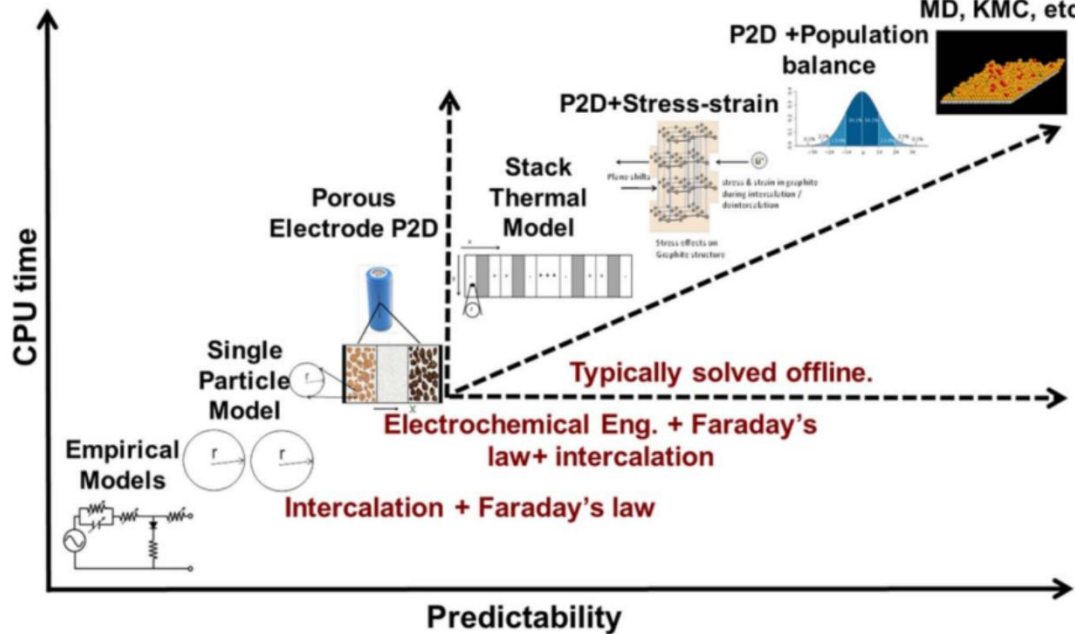
State estimation methods

Battery ageing

# 3.1 BATTERY MODELLING TECHNIQUES



Model	Complexity	Accuracy	Amount of data	Applications
PBM	high	high	low	battery design
ECM	medium	medium	high	SoH estimation
MLM	medium-high	medium	high	SoH estimation
EM	low	low-medium	high	System design & Optimization

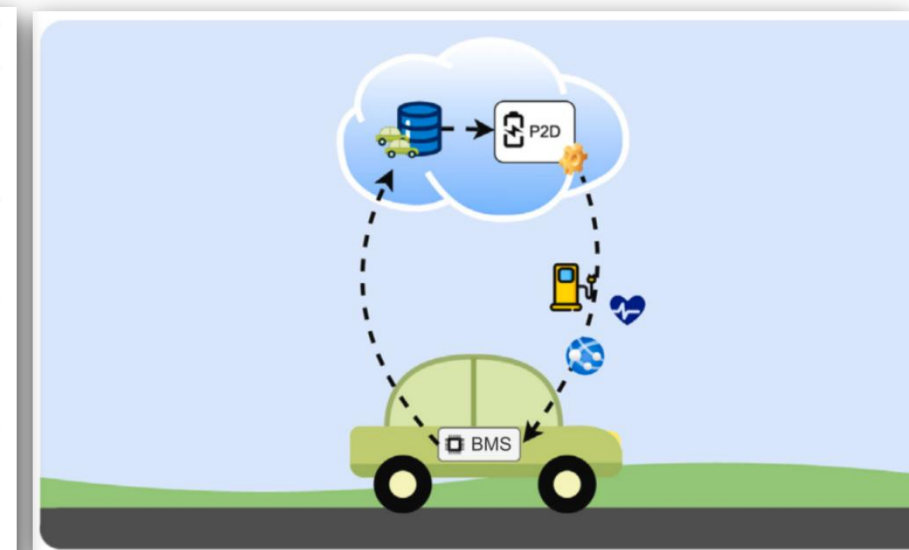


# 3.1 Modelling methods Comparison



- PBMs can achieve **high accuracy**, but they require many partial differential equations and a thorough understanding of all physical and chemical mechanisms. Furthermore, LIB aging is frequently caused by multiple factors, making **molecular modeling even more difficult** and prone to miss out on macrolevel effects. As a result, **electrochemical models** are generally **not used by nonchemical engineers/researchers**.
- ECMs model the transient response of the battery using passive circuit components, such as resistances, capacitances, and inductances. More complex models can also be used to simulate the internal diffusion and charge transfer processes. Due to their **mathematical simplicity**, they are frequently used in real-time applications, such as battery state estimations **combined with state estimators**, such as Kalman or particle filters.

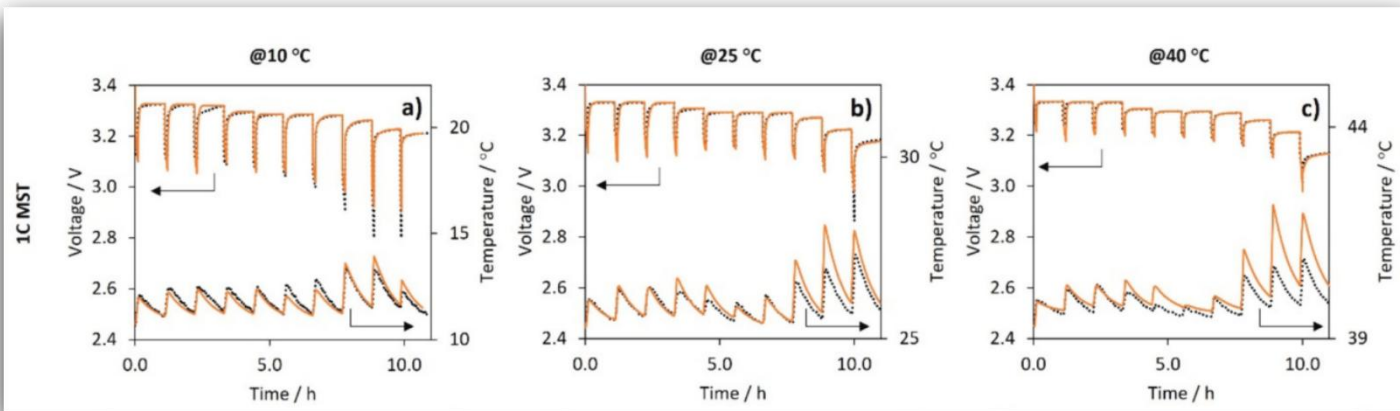
Estimation Methods	Types	Advantages	Disadvantages	Estimation Error
Experimental based [23–25]	Ampere-time counting. Open-circuit voltage. AC impedance	Simple principle. Reliable.	Time-consuming. Cannot be estimated in real time. Cumulative error exists	<5%
Model-based approaches [19,27,28]	Kalman filter. Particle filter. Sliding mode observer.	Closed-loop estimation. Low requirement for initial SOC values.	Difficult modeling. Difficult parameter identification.	<5%
Data-driven approach [21,27]	Neural network class. Support vector machine. Fuzzy logic.	No modeling is required.	High level of data dependency. Time-consuming.	<1.5%
Hybrid methods [28–32]	Data-model parallel mixture estimation. Data-model nested mixture model.	High estimation accuracy. Good robustness	Complex calculations. High energy consumption. Slow estimation speed.	<1%



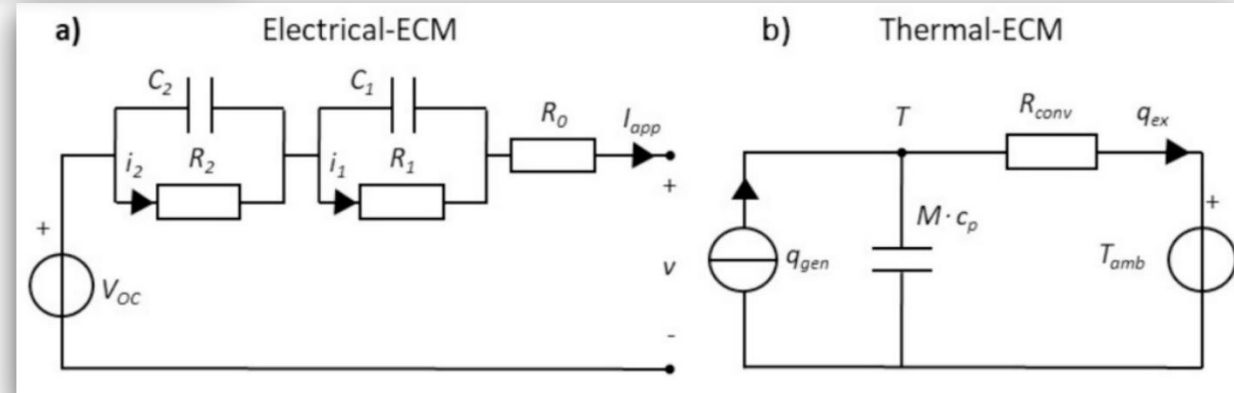
# 3.2 Electrical ECM and Thermal ECM



Among the different **Equivalent Circuit Models**, the most prevalent ones fall under the n-RC category, which includes the 0-RC model, the 1-RC model, and the 2-RC model.



Test reference number	Type of test	Ambient temperature (°C)
1	Multiple step test (MST)	
2	Charge CC-CV C/2	
3	Charge CC-CV 1C	
4	Discharge CC C/3	10, 25, 40
5	Discharge CC C/2	
6	Discharge CC 1C	
7	Discharge CC 2C	
8	WLTC	10, 20



# 3.3 P2D model and lumped thermal model



## Electrochemical model framework

Electrolyte phase  $i = N, S, P$

$$\varepsilon_{ey,i} F \frac{\partial c}{\partial t} + \frac{\partial}{\partial x} (J_{conc}) = (1 - t_+) J_{ct,i}^V$$

$$J_{conc} = - \frac{\varepsilon_{ey,i}}{\tau_{ey,i}} F \tilde{D} \frac{\partial c}{\partial x}$$

$$\frac{\partial}{\partial x} (J_2) = J_{ct,i}^V$$

$$J_2 = - \frac{\varepsilon_{ey,i}}{\tau_{ey,i}} \sigma \frac{\partial \tilde{\mu}_+^*}{\partial x} + \frac{\varepsilon_{ey,i}}{\tau_{ey,i}} \sigma \frac{2RT}{F} (1 - t_+) \gamma_\pm \frac{\partial \ln c}{\partial x}$$

Interfacial equations  $i = N, P$

$$J_{ct,i}^V = J_{ct,i} A_{am,i}$$

$$J_{ct,i} = k_{ct,i} c^\alpha \left( c_{s,i}^{max} - c_{s,i} \right)^\alpha c_{s,i}^{(1-\alpha)} \left[ \exp \left( \frac{\alpha F}{RT} \eta_{ct,i} \right) - \exp \left( - \frac{(1-\alpha)F}{RT} \eta_{ct,i} \right) \right]$$

$$\eta_{ct,i} = \tilde{\mu}_{e,i}^* - \tilde{\mu}_+^* - U_{eq,i}$$

Electro-conductive phase  $i = N, P$

$$\frac{\partial}{\partial x} (J_{1,i}) = - J_{ct,i}^V$$

$$J_{1,i} = - \sigma_{e,eff,i} \frac{\partial \tilde{\mu}_{e,i}^*}{\partial x}$$

Active material phase  $i = N, P$

$$\frac{\partial c_{s,i}}{\partial t} + \frac{\partial}{\partial y} (N_{s,i}) = - \frac{2}{y} N_{s,i}$$

$$N_{s,N} = - \frac{1}{RT} \bar{D}_{s,N} c_{s,N} \frac{\partial \mu}{\partial y} \text{ valid for } N$$

$$N_{s,P} = - D_{s,P} \frac{\partial c_{s,P}}{\partial y} \text{ valid for } P$$

$$\mu = \mu_{eq} - RT a^2 \frac{\partial^2 \tilde{c}_{s,N}}{\partial y^2} \text{ valid for } N$$

## Lumped thermal model framework

$$Mc_p \frac{dT}{dt} = \dot{q}_V V_{act} - h A_{ext} (T - T_{amb})$$

$$\dot{q}_V = \left( \dot{q}_N + \dot{q}_S + \dot{q}_P \right)$$

$$\dot{q}_i = \int \left( \dot{Q}_{rev,i} + \dot{Q}_{rxn,i} + \dot{Q}_{ohm,i} \right) \frac{dx}{L_{tot}} \quad i = N, S, P \text{ and } L_{tot} = L_N + L_S + L_P$$

$$\dot{Q}_{rev,i} = J_{ct,i}^V T EHC_i \quad i = N, P$$

$$\dot{Q}_{rxn,i} = J_{ct,i}^V \eta_{ct,i} \quad i = N, P$$

$$\dot{Q}_{ohm,i} = \frac{\varepsilon_{el,i}}{\tau_{el,i}} \sigma_{el,i} \left( \frac{\partial \tilde{\mu}_{e,i}^*}{\partial x} \right)^2 + \frac{\varepsilon_{ey,i}}{\tau_{ey,i}} \sigma \left( \frac{\partial \tilde{\mu}_+^*}{\partial x} \right)^2 - \frac{\varepsilon_{ey,i}}{\tau_{ey,i}} \frac{2RT\sigma}{F} (1 - t_+) \gamma_\pm \frac{\partial \ln c}{\partial x} \frac{\partial \tilde{\mu}_+^*}{\partial x} \quad i = N, S, P$$

Transport, kinetics, and equilibrium parameters

$$U_{eq,N} = E^\circ - \frac{\mu}{F} + (T - T_{ref}) EHC_N$$

$$U_{eq,P} = U_{eq,ref,P} + (T - T_{ref}) EHC_P$$

$$D_{s,i} = D_{s,i}^\circ \exp \left( - \frac{E_{D_{s,i}}}{R} \left( \frac{1}{T} - \frac{1}{T_{ref}} \right) \right) \quad i = N, P$$

$$k_{ct,i} = k_{ct,i}^\circ \exp \left( - \frac{E_{k_{ct,i}}}{R} \left( \frac{1}{T} - \frac{1}{T_{ref}} \right) \right) \quad i = N, P$$

Boundary conditions of the PBM.

$$J_{conc}|_{x=I} = 0; J_{conc}|_{x=IV} = 0$$

$$J_2|_{x=I} = 0; J_2|_{x=IV} = 0$$

$$\tilde{\mu}_{e,N} \Big|_{x=I} = 0; J_{1,N}|_{x=II} = 0$$

$$J_{1,P}|_{x=IV} = \frac{i_{cell}}{N_{cell} A_{act}} \quad (CC)$$

$$J_{1,P}|_{x=III} = 0; \quad \tilde{\mu}_{e,P} \Big|_{x=IV} = V_{CV} \quad (CV)$$

$$J_{s,i}|_{y=0} = 0; J_{s,i}|_{y=r_i} = J_{ct,i}$$

# 3.4 Comparison between ECM and PBM



## Geometrical, microstructural, electrochemical and transport parameters of the PBM

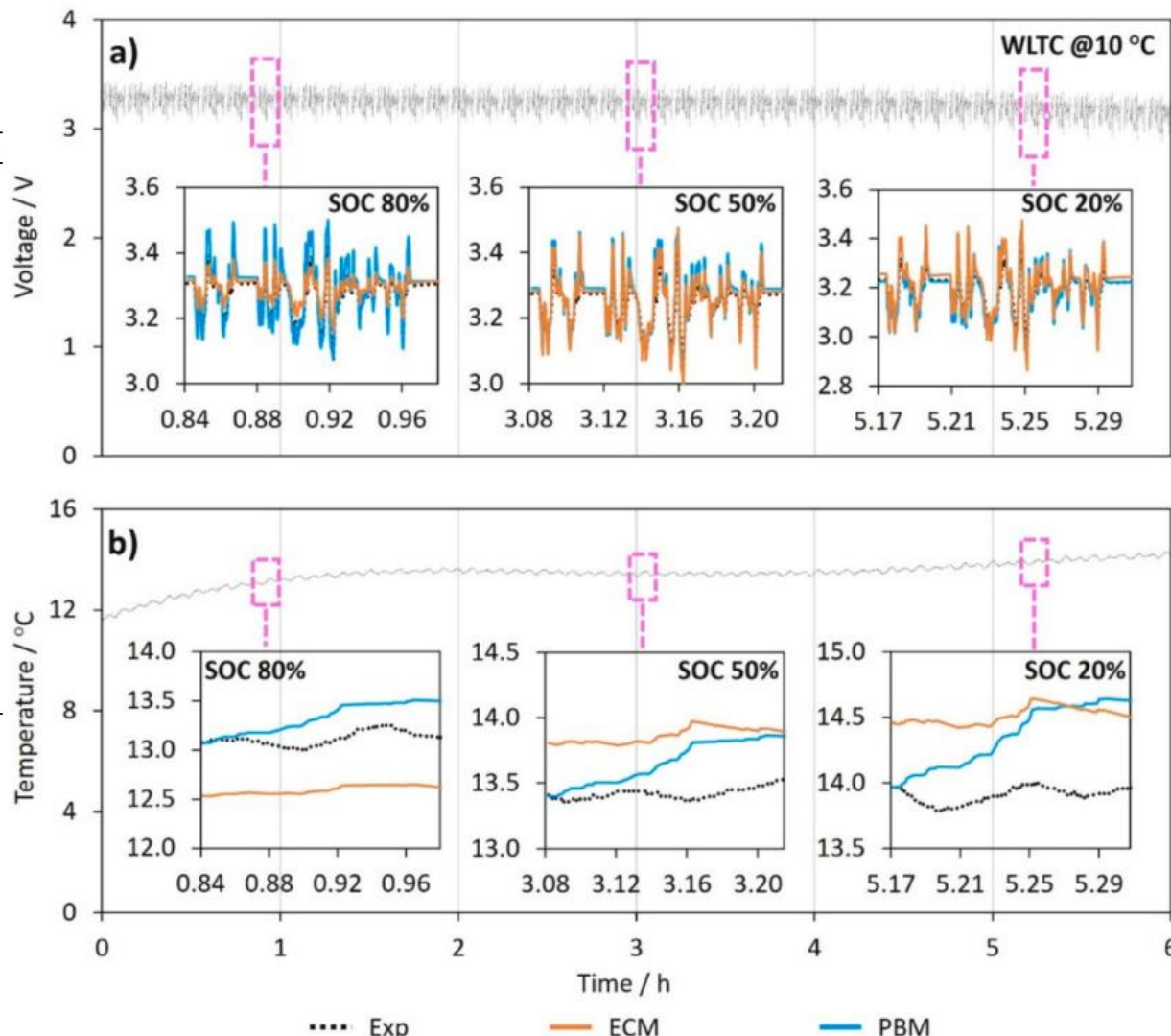
Parameter	Negative electrode (graphite)	Separator	Positive electrode (LFP)
Thickness $L$ [μm]	72.5 <sup>a</sup>	25 <sup>a</sup>	76.1 <sup>a</sup>
Particle radius $r$ [μm]	10 <sup>b</sup> [3]		0.0365 <sup>b</sup> [51,103]
Active material surface area per unit of volume $A_{am}$ [m <sup>-1</sup> ]	1.376 10 <sup>5c</sup>		3.699 10 <sup>7c</sup>
Volume fraction $\varepsilon$ [-]	$am = el = 0.463^c$ $fill = 0.057^b$ [93] $ey = 0.480^c$ $\leftarrow$ 0.5 <sup>b</sup> Table S6 <sup>d</sup> 29,920 <sup>b</sup> [30]	$fill = 0.55^c$ $ey = 0.45^b$ [78]	$am = 0.450^c$ $fill + el = 0.1^b$ [91] $ey = 0.450^c$ $\rightarrow$ 0.5 <sup>b</sup> Table S6 <sup>d</sup> 22,806 <sup>b</sup> [10,103]
Bruggeman factor $\beta$ [-]			Eq. (S2) <sup>b</sup> [92]
Symmetry factor $\alpha$ [-]			-
Kinetic constant $k_a^o$ [A m <sup>-2</sup> ]			Table S5 <sup>b</sup> [100]
Maximum Li concentration $c_s^{max}$ [mol m <sup>-3</sup> ]			Min = 0.03 <sup>b</sup> Max = 0.90 <sup>b</sup>
Open circuit potential $U_{eq}$ [V]	Eqs. (S1a)–(S1g) <sup>b</sup> [3]		6.75 <sup>b</sup> [96]
Characteristic interface length $a$ [μm]	0.316 <sup>b</sup> [3]		Table S8 <sup>d</sup>
Standard potential of intercalated Li $E'$ [V]	0.136 <sup>b</sup> [3]		30,000 <sup>d</sup>
Entropic heat coefficient $EHC$ [V K <sup>-1</sup> ]	Table S4 <sup>b</sup> [68]		50,000 <sup>d</sup>
Min/Max state of lithiation $\tilde{c}_s^{min/max}$ [-]	Min = 0.04 <sup>b</sup> Max = 0.73 <sup>b</sup> 10 <sup>b</sup> [3]		
Solid-phase conductivity $\sigma_d$ [S m <sup>-1</sup> ]	Table S7 <sup>d</sup> [3]		
Solid-phase diffusivity $D_s^o / \bar{D}_s$ [m <sup>2</sup> s <sup>-1</sup> ]	20,000 <sup>d</sup>		
Charge-transfer constant activation energy $E_{ktu}$ [J mol <sup>-1</sup> ]	45,000 <sup>d</sup>		
Solid-phase diffusion activation energy $E_{D_u}$ [J mol <sup>-1</sup> ]			
Initial electrolyte concentration $c^{in}$ [mol m <sup>-3</sup> ]	←	1000 <sup>b</sup> [78]	
Transference number of positive charges $t_+$ [-]	←	0.38 <sup>b</sup> [95]	
Ambipolar diffusivity $\bar{D}$ [m <sup>2</sup> s <sup>-1</sup> ]	←	Eq. (S3) <sup>b</sup> [95]	
Ionic conductivity $\sigma$ [S m <sup>-1</sup> ]	←	Eq. (S4) <sup>b</sup> [95]	
Thermodynamic factor $\gamma_{\pm}$ [-]	←	Eq. (S5) <sup>b</sup> [95]	
Heat transfer coefficient $h$ [W m <sup>-2</sup> K <sup>-1</sup> ]	20 <sup>a</sup> [51]		
Equivalent specific heat $c_p$ [J kg <sup>-1</sup> K <sup>-1</sup> ]	1600 <sup>a</sup> [51]		

<sup>a</sup> Measured.

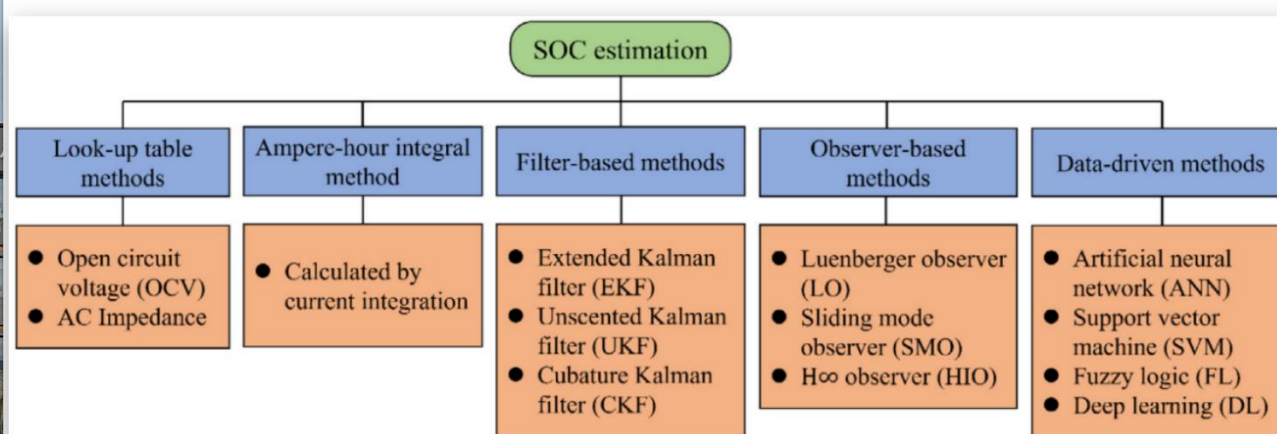
<sup>b</sup> Assumed.

<sup>c</sup> Calculated.

<sup>d</sup> Fitted to experimental data.



# 3.4 SOC and SOH estimation techniques



## State of Charge(SOC):

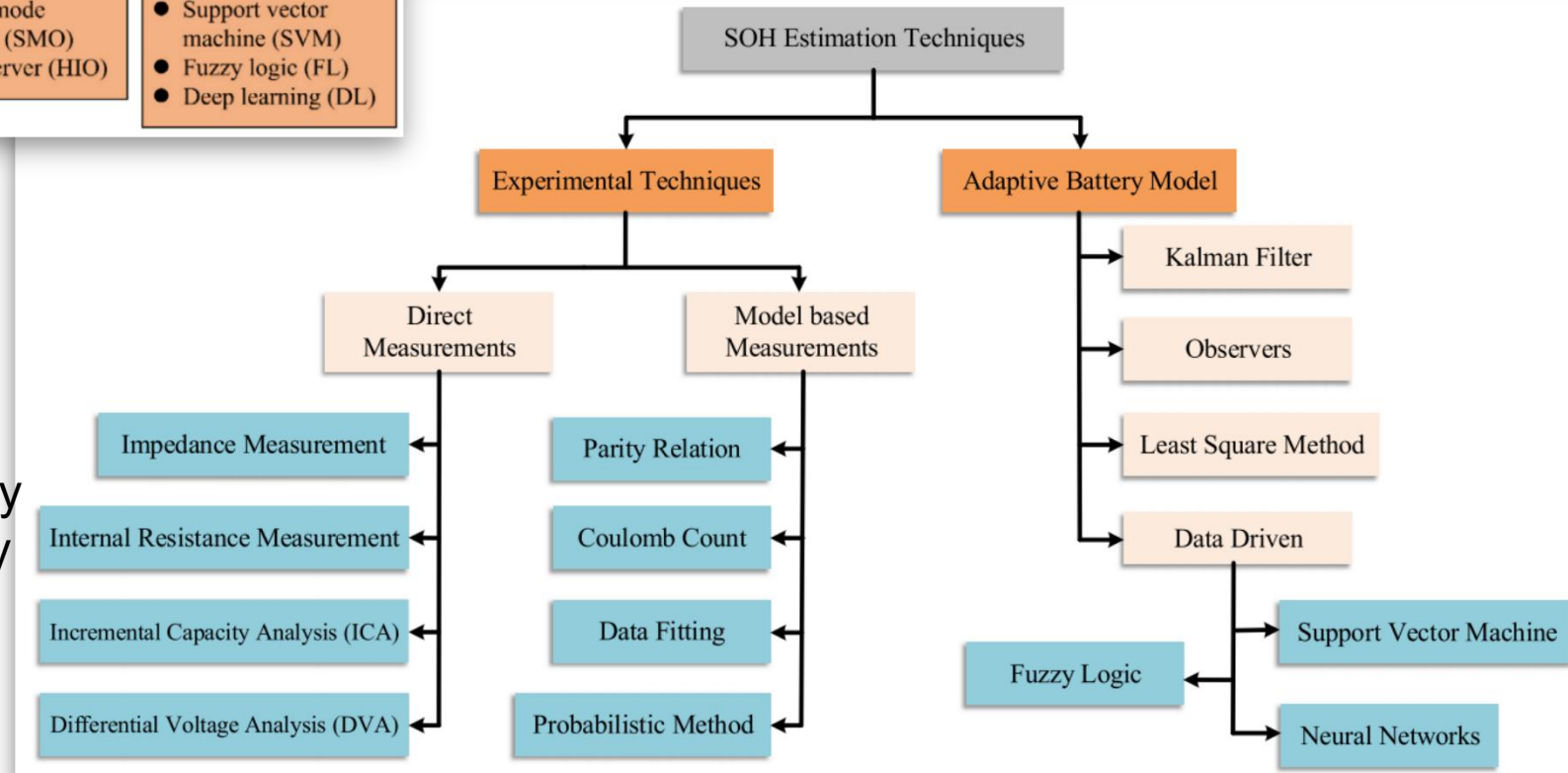
$$SOC = \frac{Q_{current}}{Q_{rate}} \times 100\%$$

$Q_{current}$  - residual capacity  
 $Q_{rate}$  - available capacity

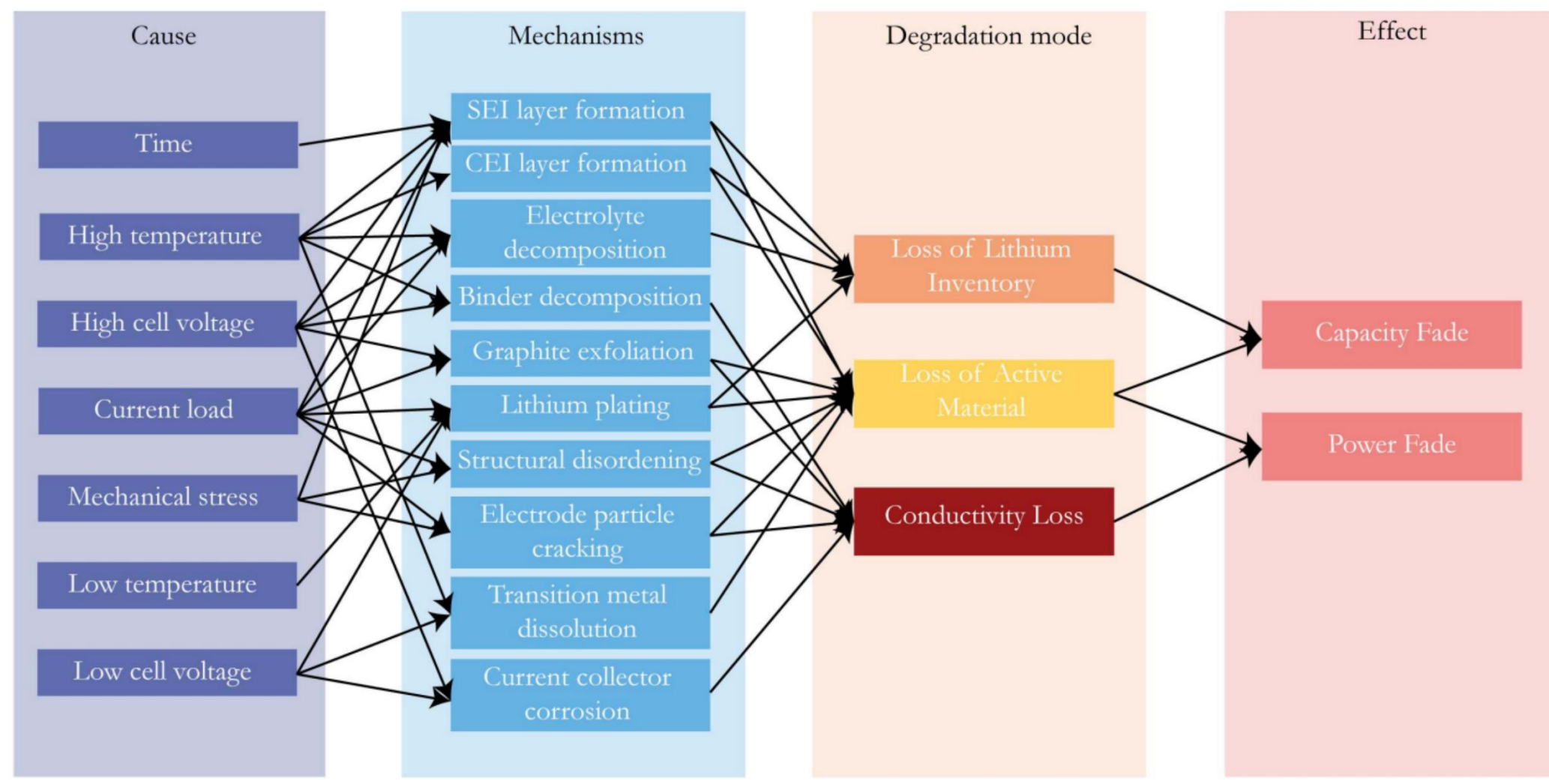
## State of Health(SOH):

$$SOH = \frac{Q_{available}}{Q_{nominal}} \times 100\%$$

$Q_{nominal}$  - Nominal capacity  
 $Q_{available}$  - available capacity



# 3.5 Battery Ageing



### 3.5 Battery Degradation Modes



- Loss of Lithium Inventory (LLI): It represents the **loss of active lithium ions** that are no longer available for cycling. Causes for LLI can be parasitic side reactions, such as surface film formation, decomposition reactions, and lithium plating, among other things. LLI is associated with capacity fade, i.e., the loss of effective mAh of the cell.
- 2) Loss of Active Material (LAM): It represents the loss or structural **degradation of the available anode or cathode material**. Possible causes include electrode surface layer growth or cycling-induced cracks/exfoliation. LAM can cause both power and capacity to fade.
- 3) Conductivity Loss (CL): It is also known as contact loss, describes the **degradation of electrical parts**, such as the current collector corrosion and binder decomposition.



## 4. Deep Neural Network(DNN) based states estimation

Battery modelling using Deep Learning  
DNN based states estimation framework  
Types of DNN for states estimation

# 4.1 Battery Modelling using deep learning



- In contrast to conventional **model-based methods** which establish the mapping by resorting to **physics-based models**, **deep learning methods** provide a convenient approach to learning the mapping from **vast training data**.
- Specifically, **deep learning uses a deep structure** to learn hierarchical representations from training data . This process is generally fulfilled by **neural networks** because of their flexible structure.

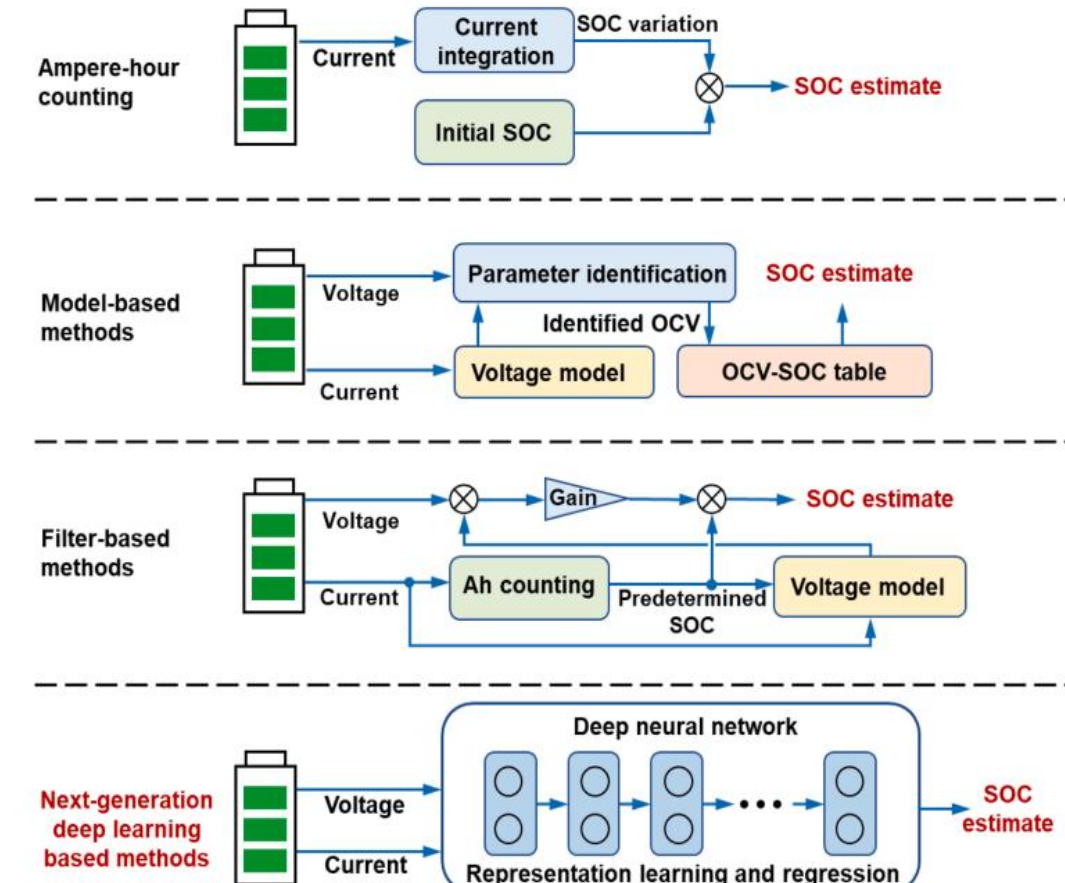


Fig. 1. Schematic diagrams of four kinds of SOC estimation methods.

# 4.2 DNN based states estimation Framework

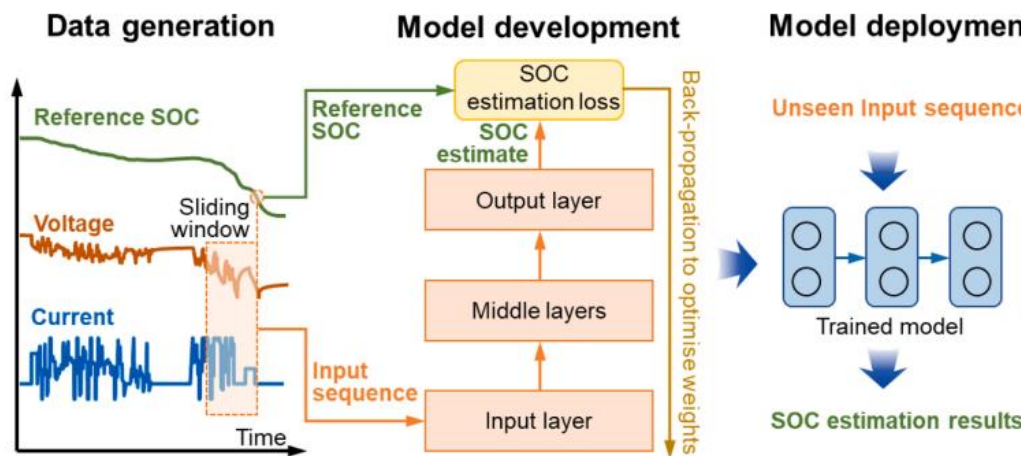
- In general, the deep learning-based SOC estimation includes **data generation, model development and model deployment** as shown in figure.
- At the time instant  $t$ , the voltage and current sequences are collected in a window with the length of  $T$ , which are then fed into a DNN to estimate SOC using eqn (\*):

$$\begin{cases} x_1 = [V_t \ L_t] \\ \hat{z}_t = f_{DNN}(x_{t-T+1:t}) \end{cases} \quad \text{--- --- (*)}$$

$x_{t-T+1}, x_{t-T+1} \dots x_t$  represents the input sequence

$f_{DNN}$  stands for mapping between the input and output

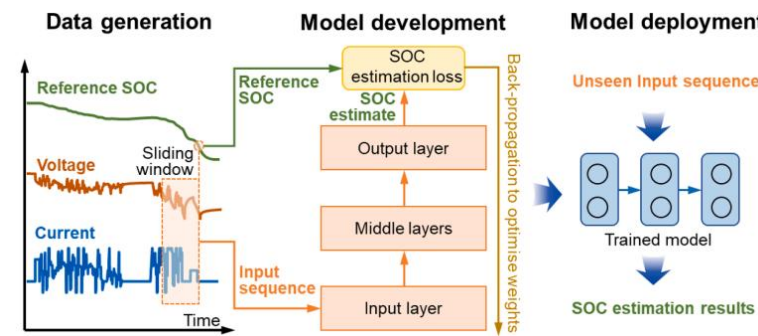
Where, V, I and  $\hat{z}$  represent voltage, current and the SOC estimation result



# STEP 1 : Data generation



- DNNs rely on a training dataset to learn the mapping
- A training dataset accommodates the voltage and current data collected from battery operations.
- The **reference SOC** is computed by resorting to **Ampere-hour counting**.
- The initial SOC can be accurately determined **by fully charging/discharging the batteries** to the upper and lower voltage limits, which correspond to the SOC of 100% and 0, respectively
- Then, the current and voltage data can be sliced together with reference SOC to **support the supervised training of a DNN**
- Existing training datasets can be classified into two types, namely **static and dynamic datasets**.



# STEP 1 : Data generation



- The static dataset considers the battery SOC estimation under a controllable condition to **rule out the impact of unseen current excitations**. For instance, battery charging is controllable in many scenarios.
- During the constant-current constant-voltage (CCCV) charging, which is a prevalent **battery charging protocol** adopted in electric vehicles (EVs). A DNN can be adopted to map the current and voltage sequence to the SOC using equation (\*).
- Once the SOC is estimated at the constant-current charging stage, the SOC is **propagated based on Ampere-hour counting** until the next charging stage.

The SOC of a battery can be updated through the following Coulomb counting equation

$$s(t) = s(0) + \frac{\eta}{3600C_{\text{batt}}} \int_0^t i(t)dt$$

where  $\eta$  is the Coulomb counting efficiency defined as follows:

$$\eta = \begin{cases} \eta_c & i(t) > 0 \\ \eta_d & i(t) < 0, \end{cases}$$

# STEP 1 : Data generation



- Additional **four advanced charging protocols**, including multistage constant current constant voltage (MCCCCV), constant power constant voltage (CPCV), alternating current (AC) and pulse charging (PC) were also adopted and the results demonstrate the **effectiveness of the DNN-based SOC estimation** under various charging conditions.
- The dynamic datasets represent more general cases where the batteries operate under **dynamic current excitations**. Such cases are prevalent in many new-energy energy storage scenarios, such as photovoltaic systems where energy generation and consumption are both dynamic
- Dynamic datasets cover different **battery materials, dynamic profiles and working conditions**, which have supported the development and validation of many DNN-based SOC estimation methods. However, as the real-world profiles depend on factors such as **driving habits, regions, and seasons**, existing datasets based on standard **driving profiles may not reflect real-world battery operations**.

Battery type	Dynamic profiles	Temperature
Panasonic 18650PF	US06, HWFET, UDDS and LA92	-20°C~25°C
LG 18650HG2	US06, HWFET, UDDS and LA92	-20°C~40°C
Turnigy Graphene 5000mAh 65C cell	US06, HWFET, UDDS and LA92	-20°C~40°C
A123 LiFePO <sub>4</sub> battery	DST and FUDS	-10°C~50°C

Public datasets containing dynamic profiles for SOC estimation

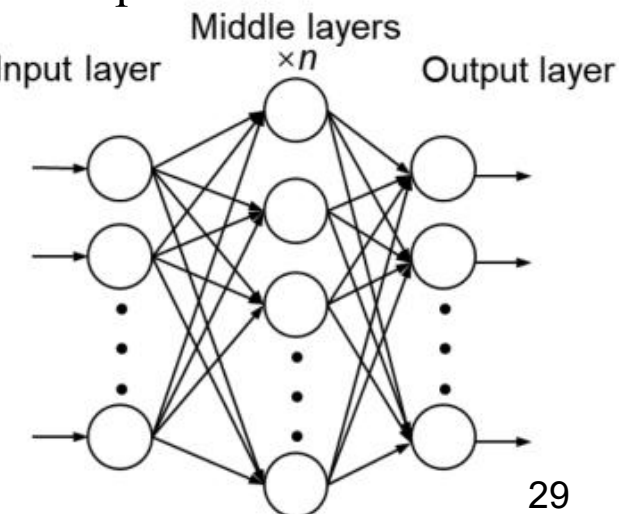
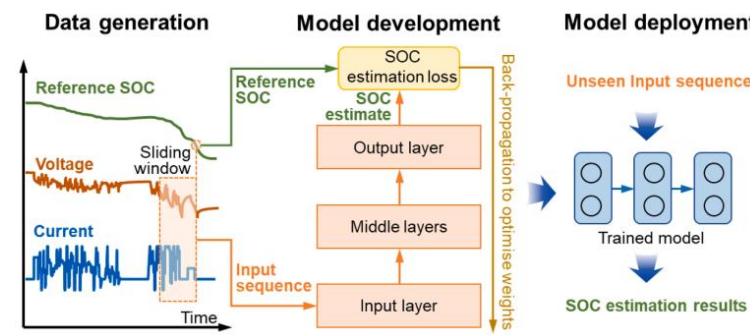
# STEP 2 : Model Development



- To learn the mapping described in Eq. (\*) from the training dataset, a DNN can be established
- It consists of an **input layer, multiple middle layers and an output layer**. The stacked layers incorporate representation learning and sequential data regression, offering high flexibility in handling various types of data.
- The model performance heavily **depends on the layer and model structures**.

$$\begin{cases} x_1 = [V_t \ L_t] \\ \hat{z}_t = f_{DNN}(x_{t-T+1:t}) \end{cases} \quad \begin{matrix} x_{t-T+1}, x_{t-T+1} \dots x_t \text{ represents the input sequence} \\ f_{DNN} \text{ stands for mapping between the input and output} \end{matrix}$$

Where, V, I and  $\hat{z}$  represent voltage, current and the SOC estimation result



# STEP 2 : Model Development



- Once a DNN is developed, it is **usually parameterised** in a supervised fashion. Weights in each layer are optimised by minimising the discrepancy between the SOC estimate and experimentally obtained reference SOC:

$$\theta_{DNN} = \arg \min f_{loss}(z, \hat{z})$$

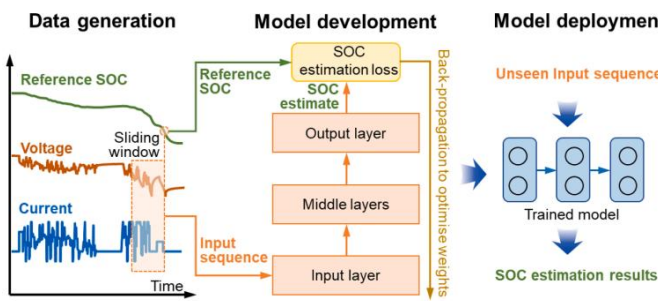
- where  $z$  and  $\hat{z}$  are the reference SOC and estimate, respectively.  $f_{loss}$  is the loss function measuring the difference between the estimation results and reference
- In the context of battery SOC estimation, **a variety of loss functions can be adopted**, such as the **mean squared error (MSE)** and **mean squared error (MAE)**. The minimisation problem is addressed through backpropagation , i.e., parameters are updated using the following rule:

$$\theta_{DNN} \leftarrow \eta \frac{\partial f_{loss}(z, \hat{z})}{\partial \theta_{DNN}} \quad \text{where, } \eta \text{ denotes learning rate}$$

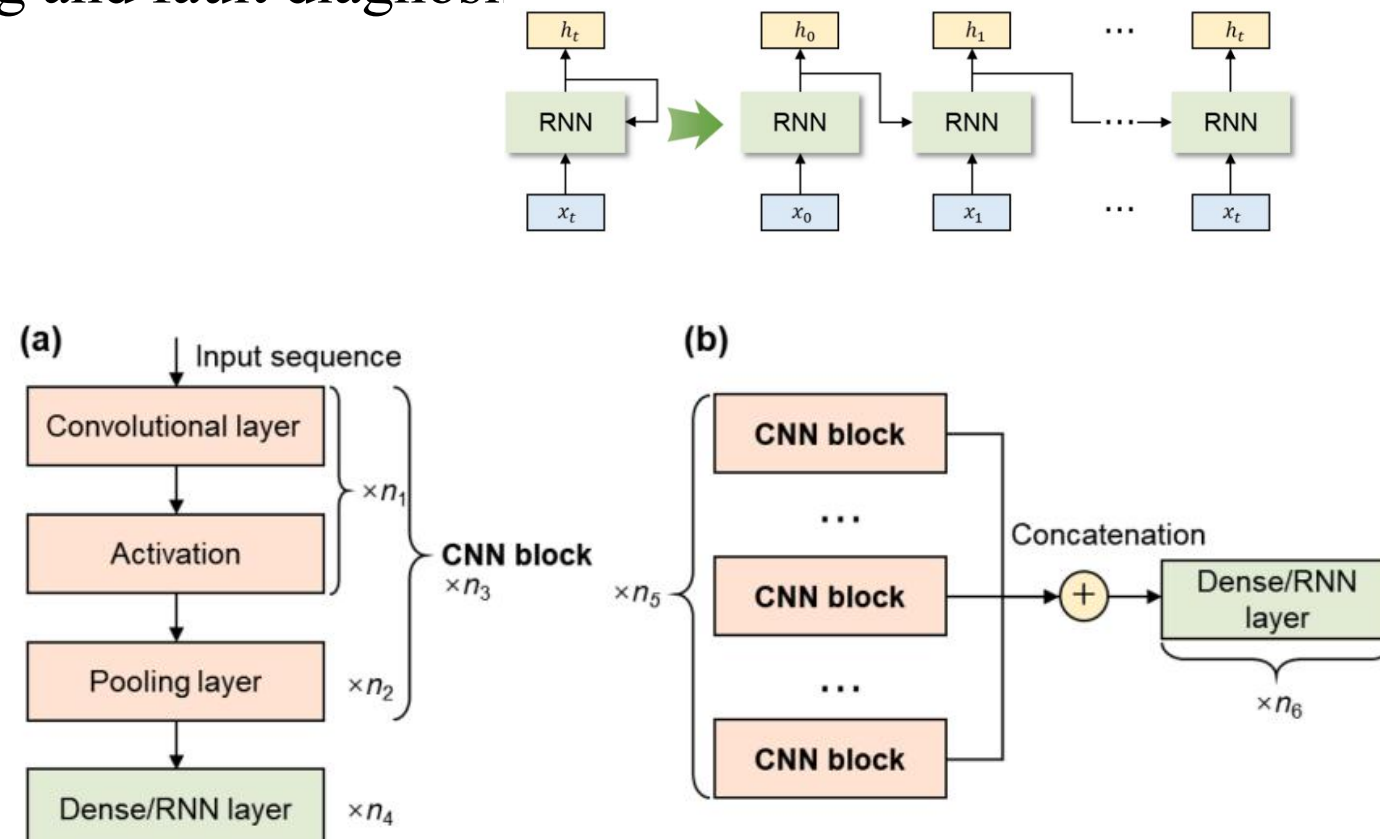
# STEP 3 : Model Deployment



- The trained DNN model can be deployed in a BMS to estimate SOC from pieces of voltage and current data. The estimation results can serve as the basis for other battery management tasks such as battery charging and fault diagnosis



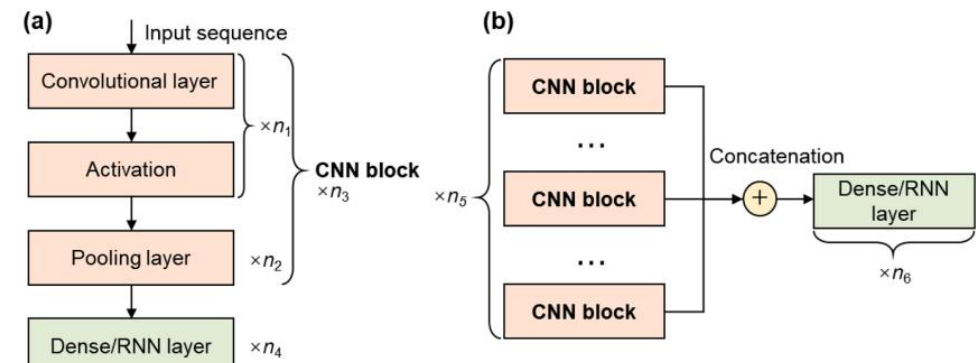
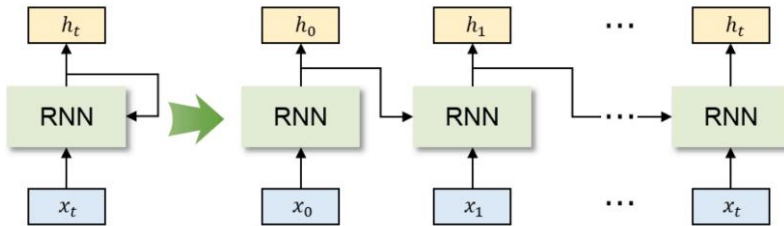
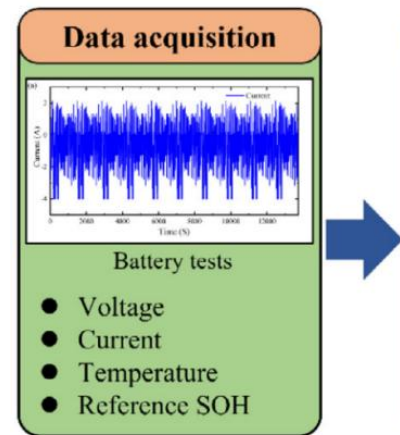
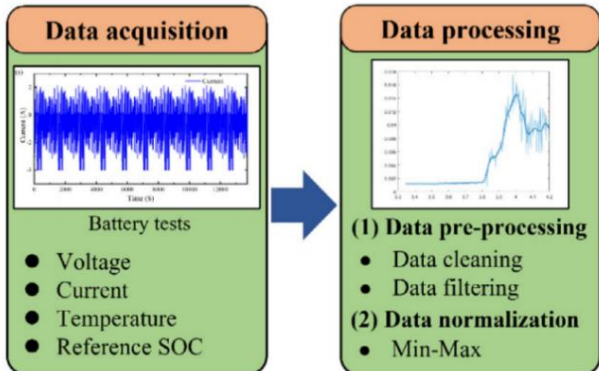
Structure and training strategy of a deep neural network for SOC estimation.



# 4.3 Types of DNN for States estimation



1. Fully connected neural networks(FCNN)
2. Recurrent neural network(RNN)
3. LSTM, GRU
4. Convolutional neural networks (CNN)

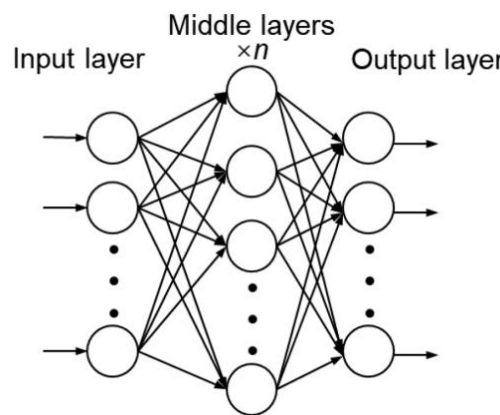


# Fully Connected Neural Networks(FCNN)



- The FCNN is one of the **most prevalent DNNs**, and its structure. In an FCNN, **each neuron in one layer is connected to all neurons in the next layer**. Accordingly, the output of the  $k$ th neuron in the  $l$ th layer is
  - where  $y_k^{(l)}$  is the output of the  $k^{th}$  unit in the  $l^{th}$  layer
  - $w_{j,k}^{(l)}$ ,  $b_{j,k}^l$  are the weight and bias between the  $j^{th}$  neuron in the  $(l-1)^{th}$  layer and the  $k^{th}$  neuron in the  $l^{th}$  layer
  - $f_a(\cdot)$  denotes an activation function, such as the rectified linear unit (ReLU), which is expressed as  $f_a(x) = \max(x, 0)$ .
- The present SOC is modelled as a function of the present voltage, current, temperature and the average current and voltage over 400 precedent time steps.
- Shows **high accuracy** under various temperatures but the fully connected structure comprises a large number of parameters gives rise to **high computational costs and overfitting risk**.

$$y_k^{(l)} = f_a \left( \sum_j w_{j,k}^{(l)} y_j^{(l-1)} + b_{j,k}^l \right)$$



# Recurrent Neural Network(RNN)

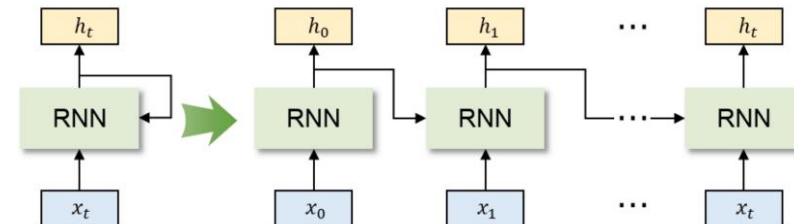


- As the **current and voltage signals** are typically **sampled as a time sequence**, RNNs have been widely employed to estimate battery SOC to take advantage of their intrinsic **capability of processing sequence dependent data**. Different from FCNNs where time dependency is not accommodated, in an RNN layer, a hidden state  $h$  is introduced to transfer information over time steps.
- We use  $x_{1:T} = (x_1, x_2, \dots, x_T)$  to replace  $x_{t-T+1:t}$  in Eq.(\*) thus the SOC estimation can be rewritten as:

$$\hat{z}_t = f_{DNN}(x_{1:T})$$

$$h_t = f_{RNN}(x_t, h_{t-1})$$

- The RNN layer **utilises a state to retain information regarding the input sequence**,
- where  $h_t \in R^D$  is a D-dimensional state vector,  $x_t \in R^M$  is an M-dimensional input vector.  $f_{RNN}$  denotes a nonlinear function described by an RNN unit.
- the simplest RNN has a sequential structure, which is given as
- $$h_t = \tanh(w_h h_{t-1} + w_x x_t + b) \text{ where, } \tanh(x) = \frac{\exp(x) - \exp(-x)}{\exp(x) + \exp(-x)}$$
- $w_h \in R^{D \times D}$  and  $w_x \in R^{D \times M}$  are two weight matrices.  $b$  is a bias matrix
- We obtain the last state vector  $h_T$  as a representation of the input sequence. Afterwards, the state vector  $h_T$  can be mapped to the target SOC:  $\hat{z}_t = g(h_T)$ , where  $g()$  denotes the nonlinear mapping between  $h_T$  and the SOC prediction result
- The results indicate the **superior performance** of RNNs in comparison with FCNNs





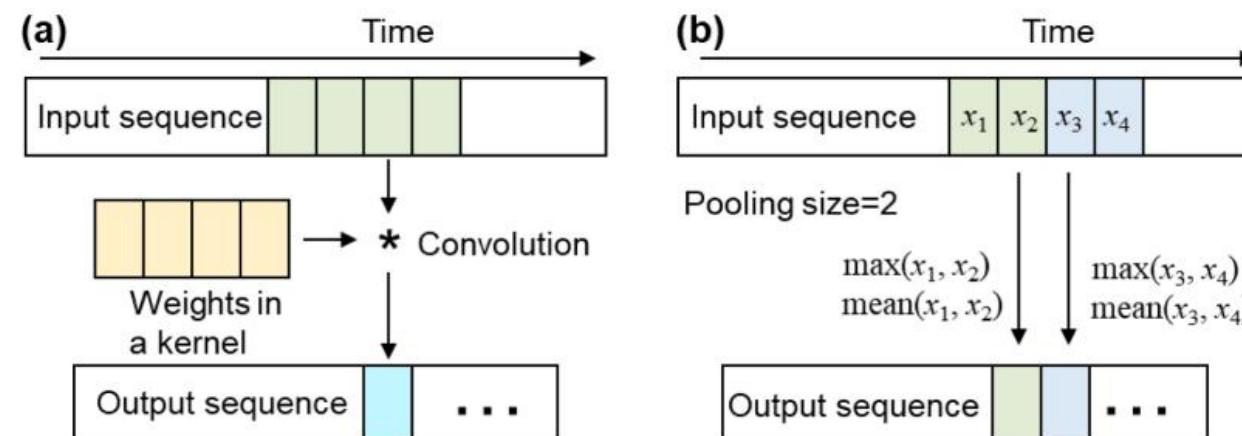
Other more advanced RNN include:

- LSTM(long short-term memory) RNN has **high capability in processing long sequences**, and it has been reported to demonstrate high accuracy in time series prediction , machine translation and health prognosis but its **complex structure gives rise to high computational burdens**. In the context of battery SOC estimation, LSTM results show that LSTM accurately estimates the two critical battery states at the same time.
- The GRU(gated recurrent unit) RNN has **comparable performance** to the LSTM but **lower computational costs**, thanks to its simpler structure and fewer training parameters. A one-cycle learning rate policy was adopted to improve the DNN performance. Validation results demonstrate that the proposed GRU model is **more accurate and efficient** than LSTM.
- Stacked RNNs
- Bidirectional RNNs
- Encoder-decoder architecture

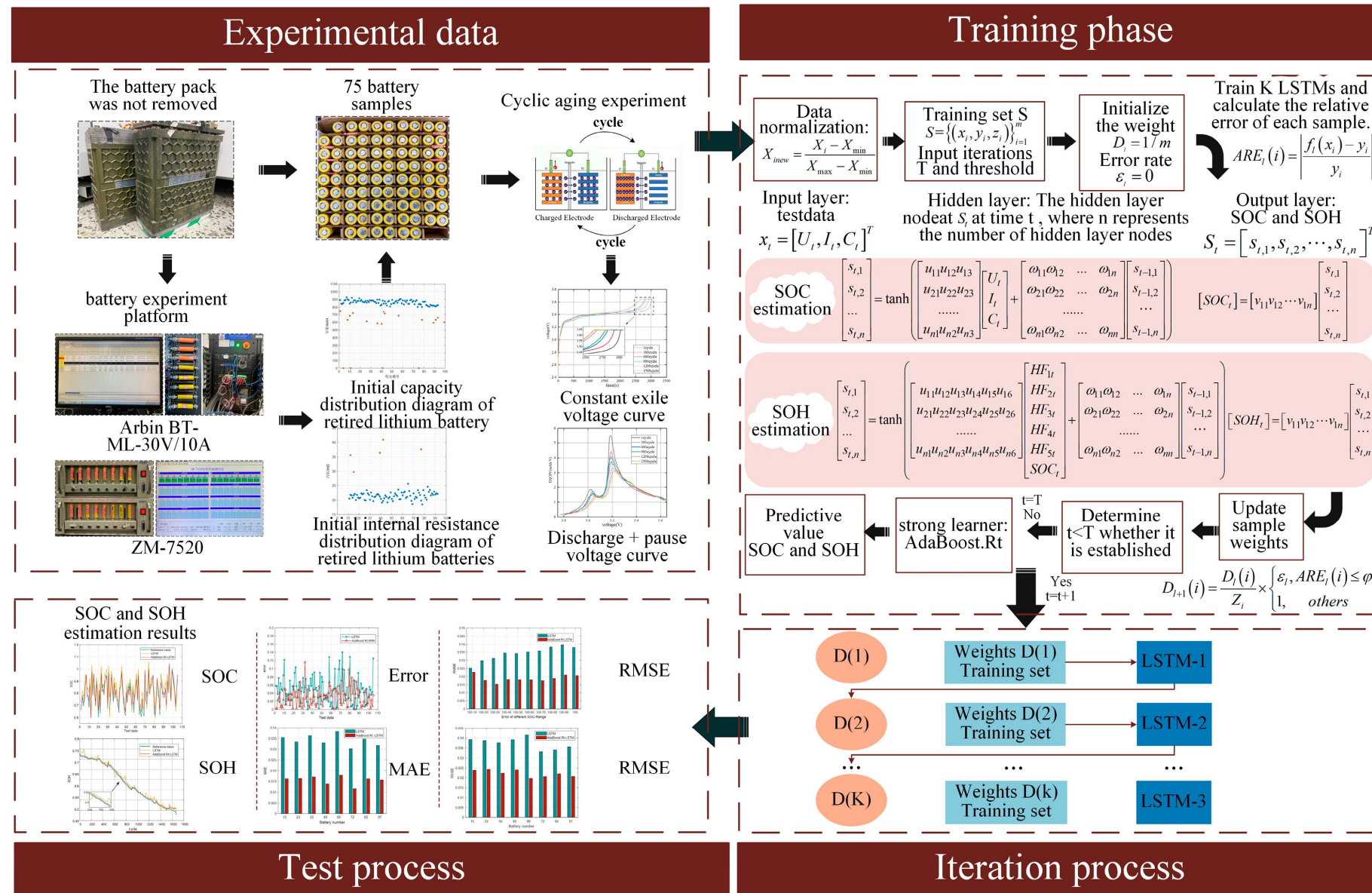
# Convolutional Neural Network(CNN)



- CNN has been rapidly applied in many fields such as **image and video processing**. In the field of battery state estimation where **sequential data** are generally studied, the 1D CNN is generally applied
- Different from the RNNs, the 1D CNN layers can process **input sequences using a set of kernels** in parallel. As demonstrated in *Fig. (a)*, each kernel utilises a sliding window to sample from the input sequence and compute the weighted sum as the element of the output sequence.
- The pooling layer provides a **down sampling method** to extract features from a convolutional layer, the commonly used down-sampling method includes **max pooling and average pooling**.
- The pooling layer can **reduce computational costs and help alleviate over-fitting** by reducing the dimension of input data. An example of the mean and maximum pooling is shown in *Fig. (b)*



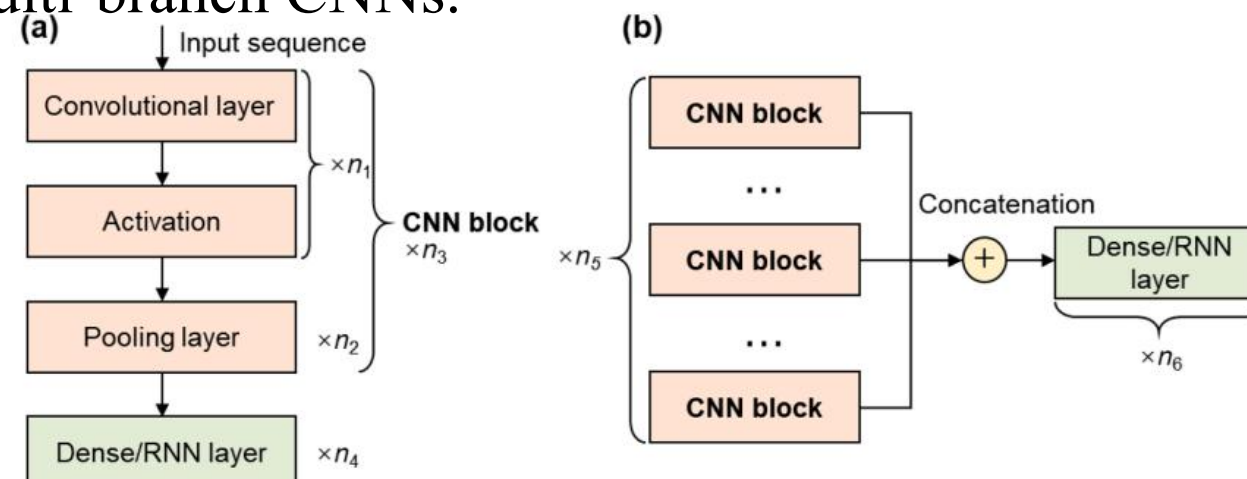
# LSTM based SOC and SOH estimation process



# Convolutinal Neural Network



- Three CNN branches consist of convolutional layers, pooling layers and fully connected layers.
- Due to **different kernel sizes** in convolutional layers, the branches **can capture long and short-term temporal dependencies** in the input data.
- Two methods to merge the output of three branches was also investigated and experimentally determined the best choice. Experimental results confirmed the reliable prediction results under common and noisy conditions. Fig. below gives a visual comparison between the single-branch and multi-branch CNNs.



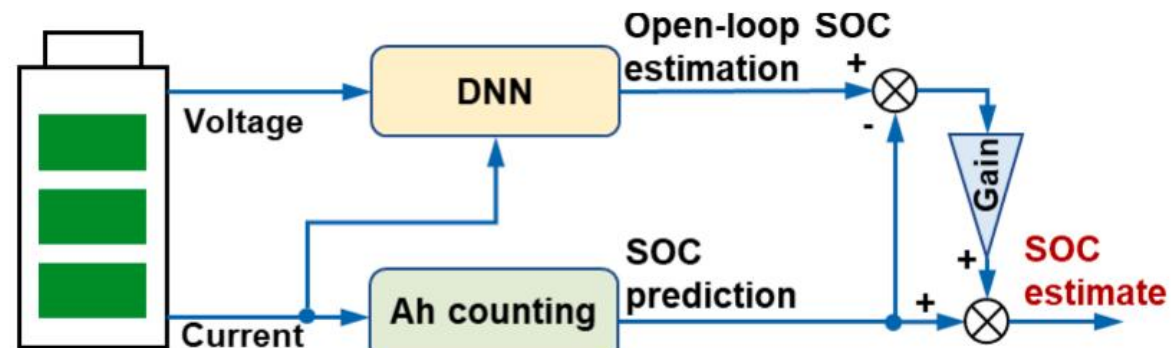
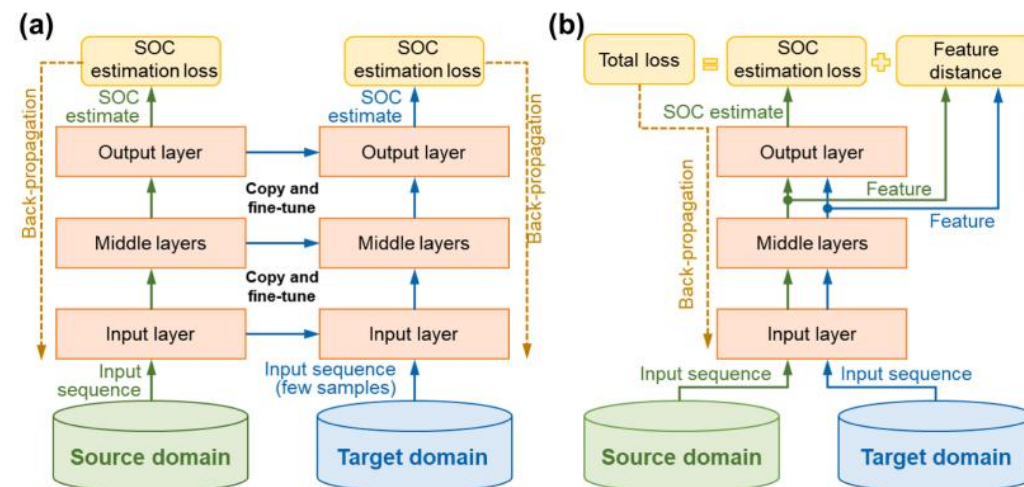
Schematic diagram of (a) single-branch and (b) multi-branch CNNs.  $n_1 \sim n_6$  are integers indicating that layers/blocks can be repeated multiple times.

# Advanced application of DNN



In addition to the basic applications which use the DNNs to map battery operating data to SOC, some recent studies have contributed to advanced applications of DNNs **to enhance their SOC estimation performance**. They are:

1. Transfer learning
  - Fine tuning
  - Domain Adaptation
2. The combination of DNNs with other methods
  - Combination of DNNs and Ampere-hour counting
  - Combination of DNNs and physics-based models



# When to use Transfer learning?



- Behind the success of deep learning-based SOC estimation, there is a **critical assumption regarding** the training data that is
- However, owing to the inconsistency in cell characteristics and variations in battery operating conditions, **the assumption may not strictly hold**, leading to the “dataset shift” issue and jeopardising estimation performance.
- A straightforward solution is to **collect more data** to bridge the gap between the training dataset and real-world samples. However, this solution may incur prohibitive costs and in some cases, it may be **not practical** for research purposes.
- An **alternative** to circumvent this issue **is transfer learning**, whose effectiveness has been demonstrated in the fields of computer vision and machine fault diagnosis.

# Transfer learning



- Mathematically speaking, transfer learning defines a **source domain** to represent a **primary training dataset**, which can be expressed as:

$$D^{(s)} = \left\{ \left( \begin{matrix} x_i^{(s)} & y_i^{(s)} \end{matrix} \right) \right\}_{i=1}^{n^{(s)}} x_i^{(s)} \in X^{(s)}, y_i^{(s)} \in Y^{(s)}$$

- where  $D^{(s)}$  denotes the source domain,  $x_i^{(s)}$  and  $y_i^{(s)}$  are the input and label of the  $i^{th}$  sample in the source domain, respectively.  $X^{(s)}$  and  $Y^{(s)}$  the collections of  $x_i^{(s)}$  and  $y_i^{(s)}$  , respectively.  $n^{(s)}$  is the total number of samples in the source domain.
- On the other hand, a **target domain**  $D^{(t)}$  is defined as :

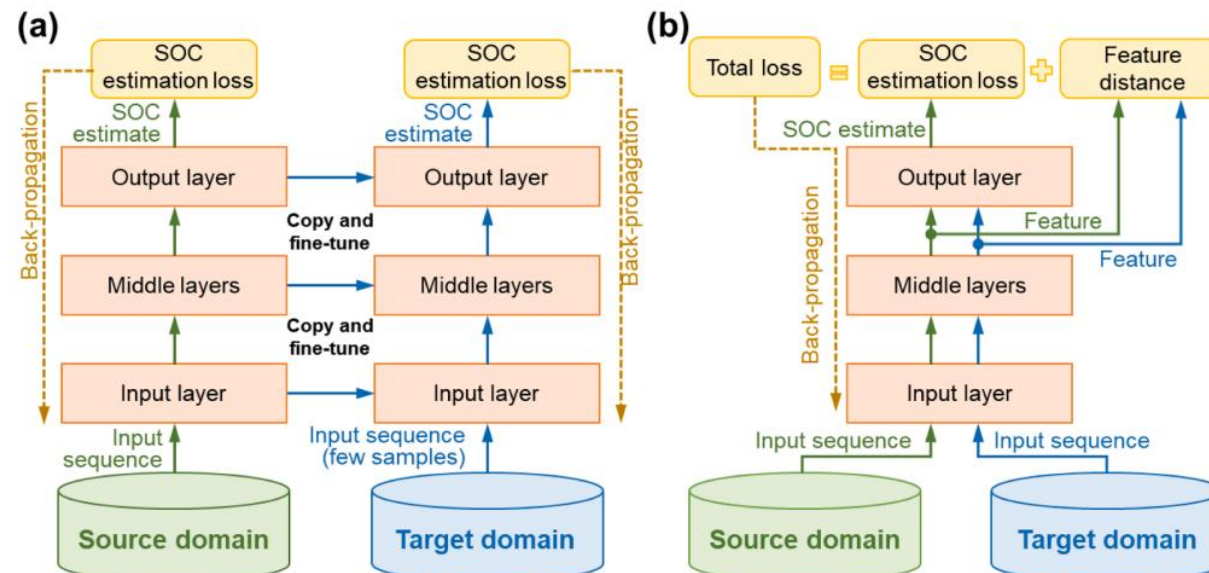
$$D^{(t)} = \left\{ \left( \begin{matrix} x_i^{(t)} & y_i^{(t)} \end{matrix} \right) \right\}_{i=1}^{n^{(t)}} x_i^{(t)} \in X^{(t)}, y_i^{(t)} \in Y^{(t)}$$

- where  $x_i^{(t)}$  and  $y_i^{(t)}$  are the input and label of the  $i^{th}$  sample in the target domain, respectively.  $X^{(t)}$  and  $Y^{(t)}$  the collections of  $x_i^{(t)}$  and  $y_i^{(t)}$  , respectively.  $n^{(t)}$  is the total number of samples in the target domain.
- The **target domain** represents the case where a trained model is intended to be used.

# Transfer learning



- The source and target domains have different probability distributions but we hope to develop a DNN to fulfil the regression task in  $D^{(t)}$ :  
$$\hat{y}_i^{(t)} = f_{DNN}(x_i^{(t)})$$
- As  $D^{(s)}$  and  $D^{(t)}$  follow different distributions, it is expected that the DNN trained on  $D^{(s)}$  to obtain  $f_{DNN}$  may not achieve satisfying results. On the other hand, the target domain  $D^{(t)}$  may consist of a few samples to support developing  $f_{DNN}$ . Consequently, it is necessary to take advantage of both  $D^{(s)}$  and  $D^{(t)}$  with transfer learning.
- As shown in Fig. below, two widely used transfer learning methods for SOC estimation are fine tuning and domain adaptation

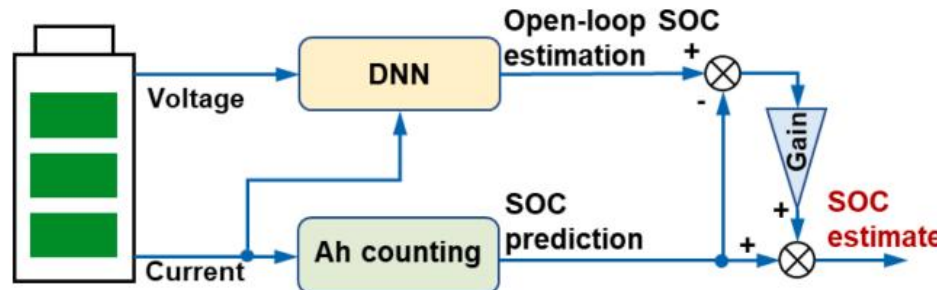


Schematic diagram of two transfer learning strategies. (a) fine-tuning and (b) domain adaptation.

# The combination of DNNs with other methods



- The combination of DNNs with other methods **aims to overcome the intrinsic limitations** of DNNs by resorting to other modelling techniques.
- The stable SOC estimation can be ensured by **the combination of DNN and Ah counting**. The validation results show that the SOC **estimation error** can be restricted to **2.03%** even in the presence of voltage plateaus of LFP batteries.
- However, this method is designed for batteries with controllable charging processes. For batteries subject to uncertain charging and discharging in solar or wind power generation systems

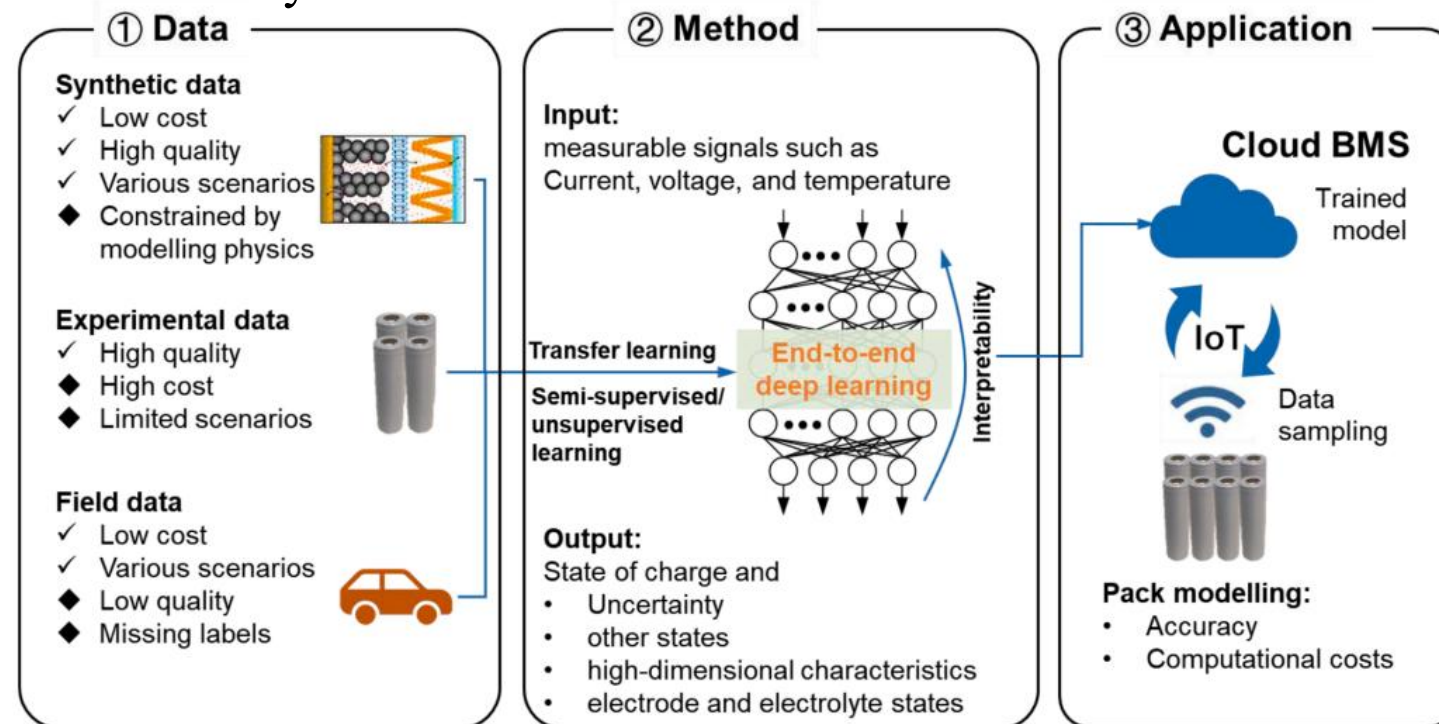


Closed-loop SOC estimation incorporating DNN-based SOC estimation  
and Ampere-hour counting

# Challanges and future of DNN



- The present SOC estimation studies are generally **based on small experimental datasets** obtained from standard EV driving profiles. In reality, battery operations are highly **dependent on many factors such as regions and driver habits**. This issue is compounded by varying battery operating conditions, such as the ambient temperature.
- Although high accuracy has been achieved even for various battery chemistries, the end-to-end modelling using **DNNs hinders the explanation of the prediction results**. As a consequence, researchers and engineers cannot judge if a DNN can perform reliably under unseen conditions.



## 5. Thesis objectives and preliminary works

Thesis objectives  
Preliminary work (experiments and simulation)  
Conclusion

# 5.1 Thesis Objectives



A. Constructing different battery modeling approaches:

- An empirical model which is known as **Equivalent Circuit Model** consist of circuit elements such as resistors and capacitors
- **Data driven Model** that depend on data collected in the lab and under various usage for better prediction of battery ageing mechanism

B. Building a simulation environment for an **electric vehicle in Matlab/Simulink** and integrating it with the battery models in Matlab for BEV simulation, which can take driving profile and ambient temperature as an input and provides **battery states SOC, SOH**, etc as an output.

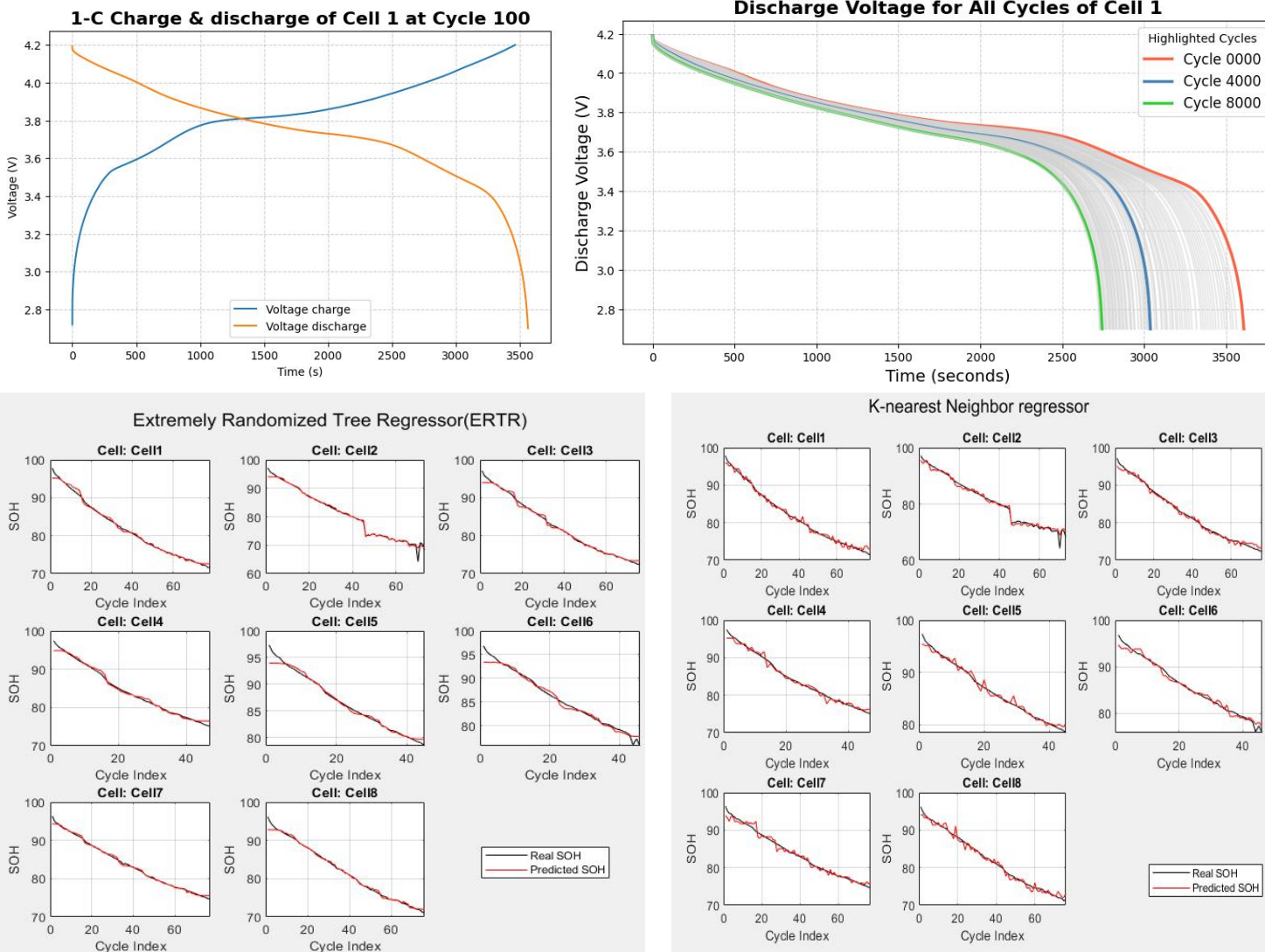
C. Accuracy **comparison** of 1-RC model, **2-RC model** and Various **Deep Learning algorithms** such as FFNN, LSTM, and implementation of the hybrid methods such as LSTM + SPKF, LSTM + ACKF, LSTM + PF etc.

# 5.2 Preliminary Work- Dataset analysis



## Oxford battery dataset

- Eight commercial Kokam pouch Cells
- 4 layers of data related to **8 cells**
- Each cell has the capacity of 740 mAh and were tested in a constant temperature environment of **40 degrees**.
- Each cell was tested using **1-C Charge/Discharge** (Standard charge and discharge at a current of 740mA) and Pseudo-OCV Charge/Discharge (A slower charging and discharging process at 40mA)
- Contains detailed measurements for each cycle including time, voltage, charge, and temperature for every 100 drive cycles (a total of **about 8000 cycles** for each cell)



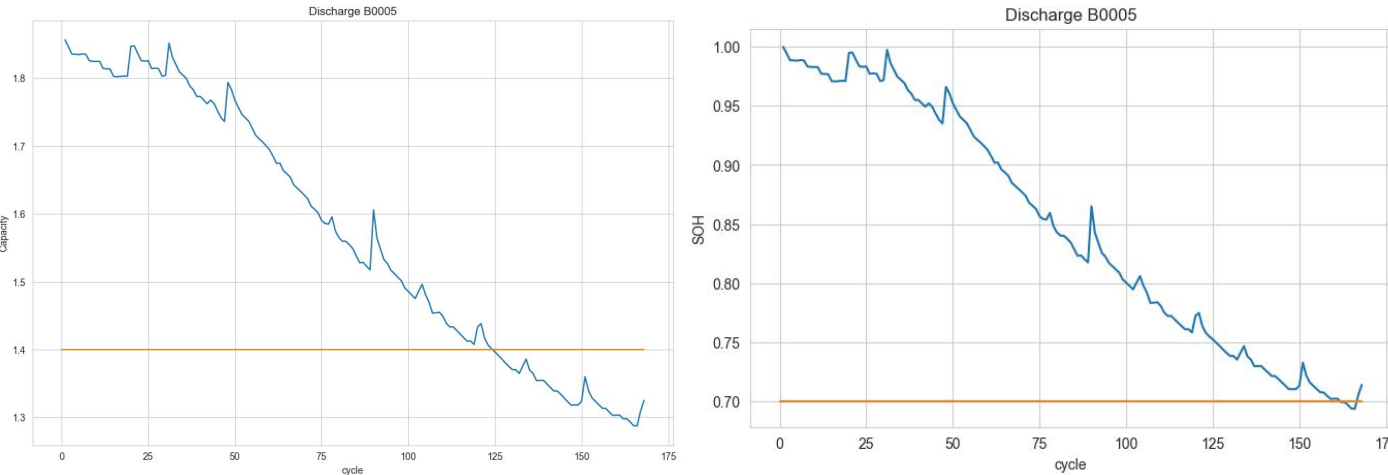
# 5.2 Preliminary Work- Dataset analysis



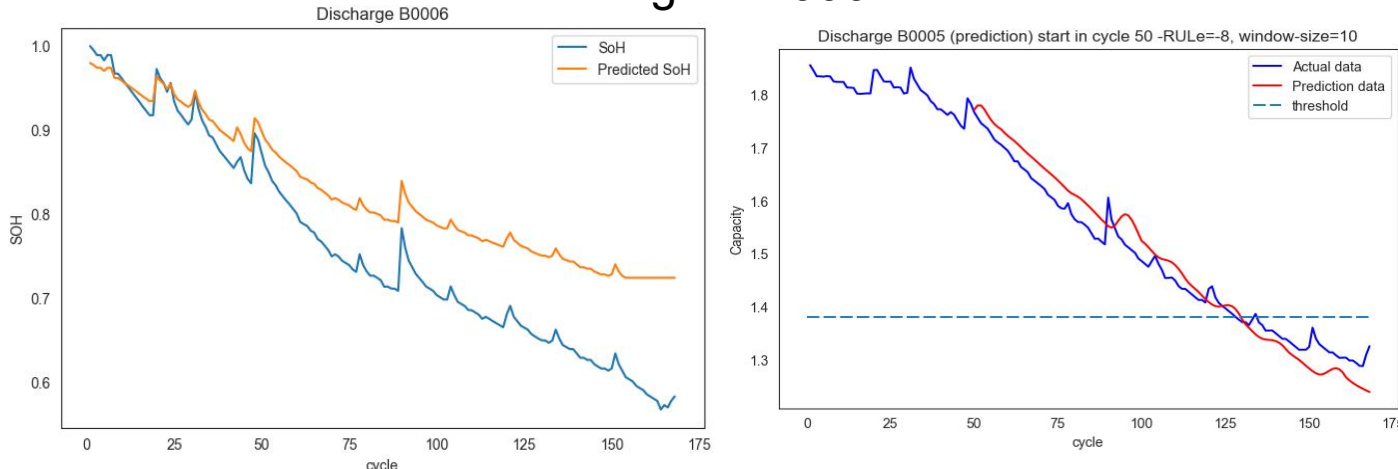
## NASA Battery Dataset

- Batteries were Li-ion cells that were placed through **about 200 charge, discharge, and impedance pulse cycles** to show the aging effects.
- Charging was done by constant current (CC) mode at  $1.5A$  until  $4.5V$  was reached. This voltage was held in Constant Voltage(CV) mode until the current tapered to  $20mA$ .
- Discharging was done through CC at  $2A$  until the battery voltage fell between  $2.2V - 2.5V$  depending on the battery cell.
- Impedance measurements were carried out through **Electrochemical Impedance Spectroscopy(EIS)**
- Experiment stopped once EUL criteria of  $1.4 Ahr$  capacity was met

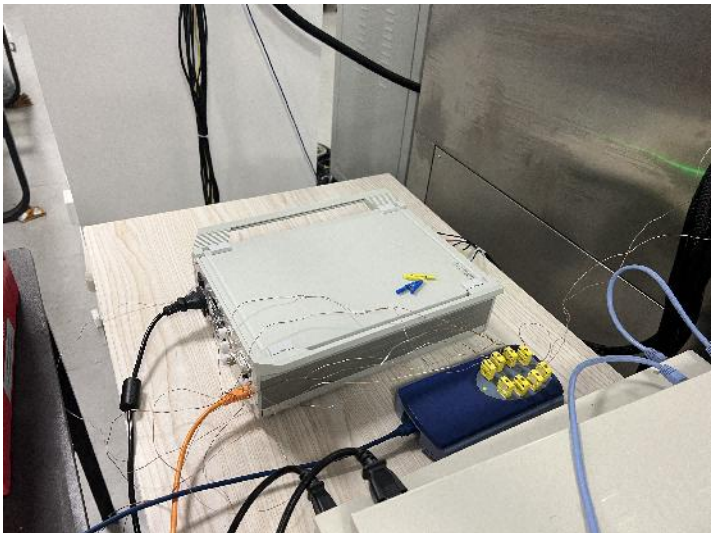
Training and testing on B005 batch size=25, epochs=50



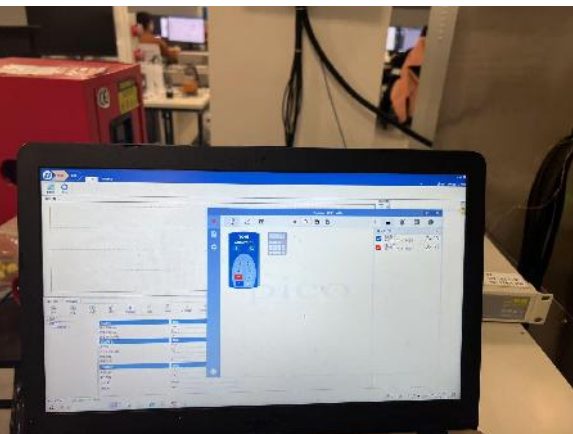
Testing on B006



# 5.2 EIS experiment Equipments



EIS and temperatur measurement



Data acquisition computer



Temperature  
controled chamber



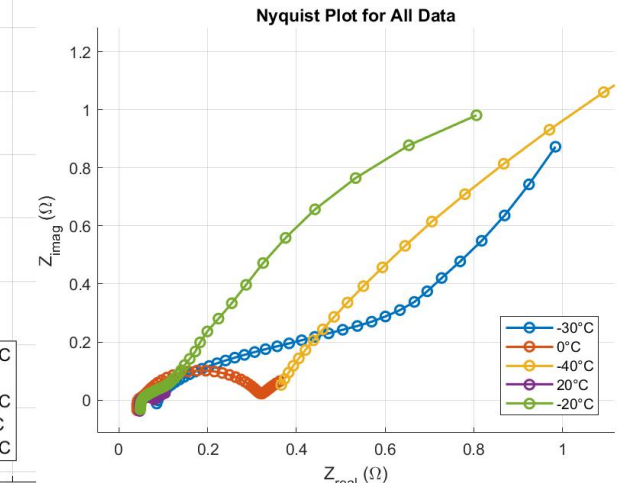
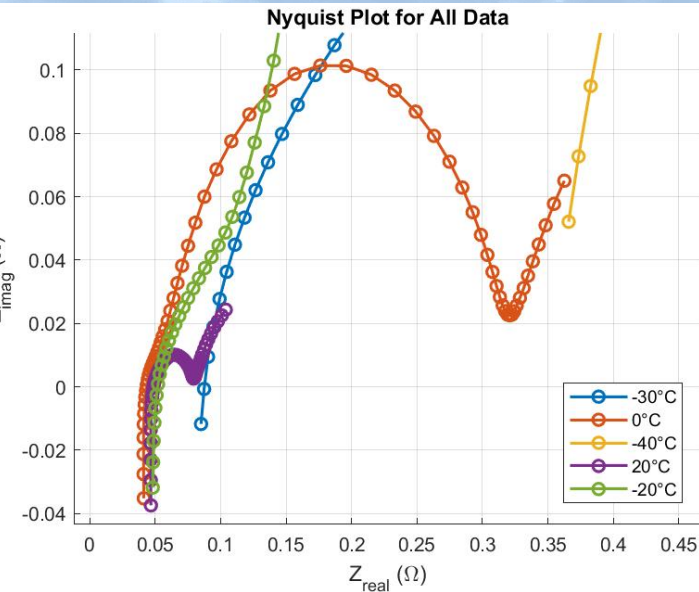
6000 mAh pouch  
cell

# 5.2 EIS experiments data analysis



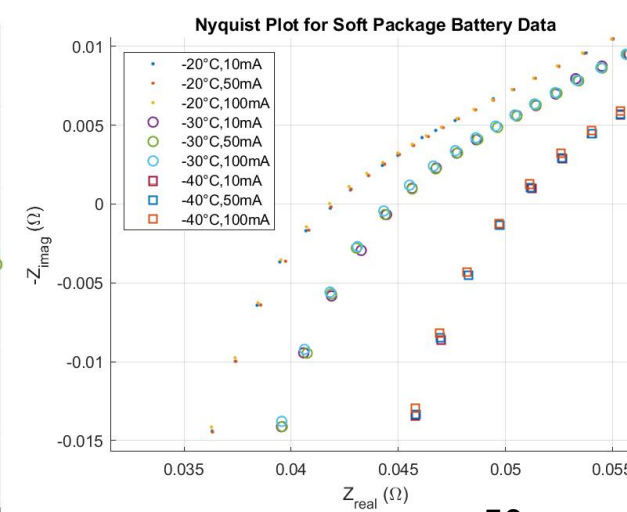
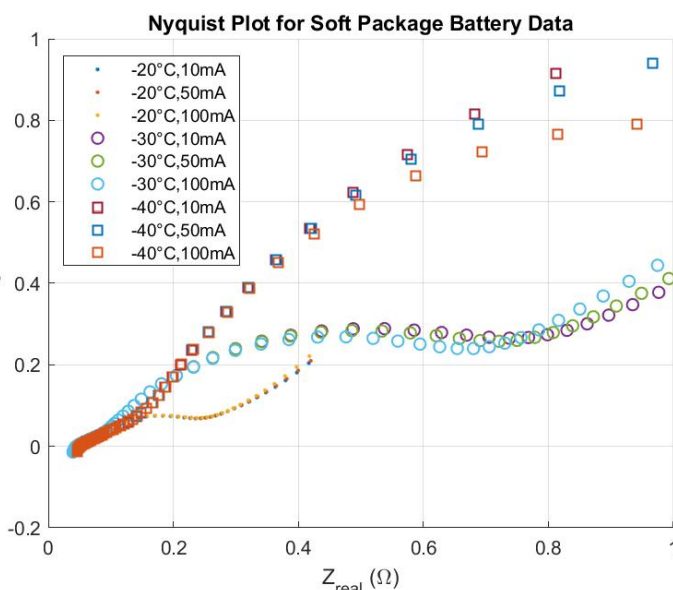
## Cylindrical Cell

- Cell performs well at 20 degrees and even in 0 degrees but poorly in -20 degrees and below

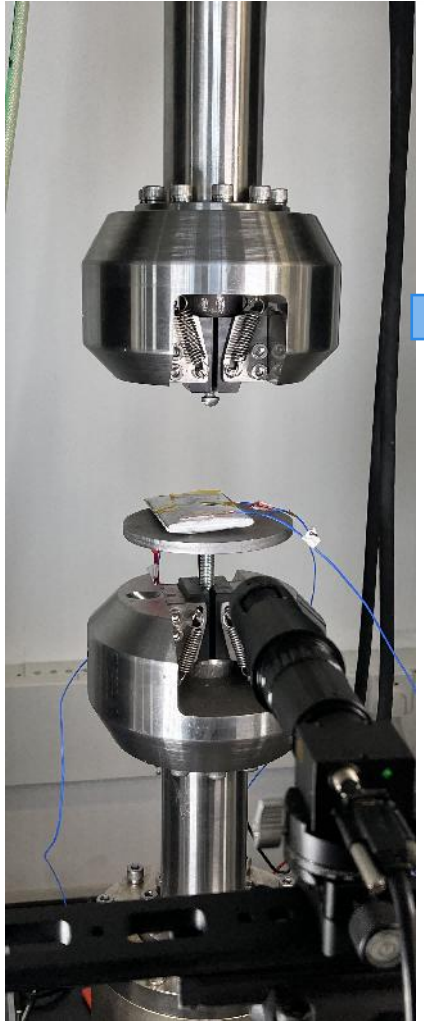


## Pouch Cell

- Cell performs well at -20 but poorly in -30 Degrees and -40 Degrees



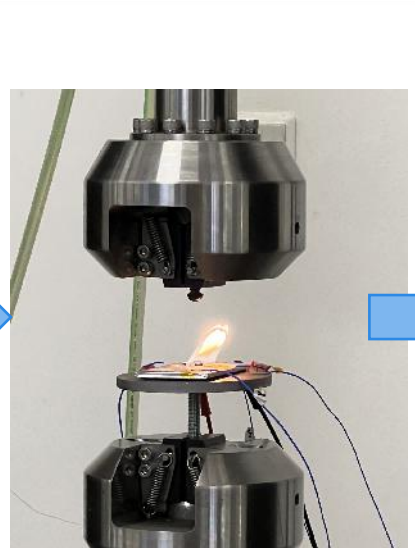
# 5.2 Other works- Battery Stress test



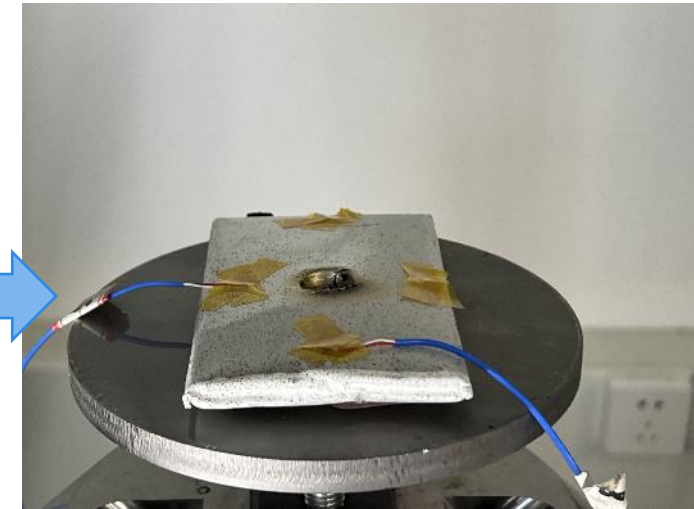
Test setup



During test



After 5mm penetration the cell is dead



Force applied vs Penetration distance



Infrared Camera

## 5.3 Conclusion



- Relevant literature review of various battery modelling techniques
- BMS is responsible for better battery performance, longevity, and protection from damage.
- Equivalent circuit model is the most famous and widely used battery modelling technique.
- Electrochemical model can produce high accuracy state prediction with various internal cell parameters but it is computationally expensive and fairly difficult to start.
- **Data driven battery** modelling technique is also known as ‘black box model’ but shows promising results . It offers easy to start modelling but highly **dependent on training data** from experiments.
- Thus, **lots of experiments like battery cycling, Electrochemical Impedance Spectroscopy are needed** to model the commercially availabe Lithium ion batteries.
- **Focus on developing accurate Data Driven Model and implement in Matlab/simulink environment for EV simulation considering different driving profiles and ambient temperatures**



End of the presentation!

Thank you for your attention!

Dhakal Amrit

Thesis Proposal Defense

Master of Science in Aeronautical and Astronautical Technologies

School of Civil Aviation

Northwestern Polytechnical University